DATA ACQUISITION AND CONTROLS FOR HALL EFFECT THRUSTERS

by

JOHN J. MANKOWSKI, B.S.E.E.

A THESIS

IN

ELECTRICAL ENGINEERING

Submitted to the Graduate Faculty
of Texas Tech University in
Partial Fulfillment of
the Requirements for
the Degree of

MASTER OF SCIENCE

IN

ELECTRICAL ENGINEERING

Approved

May, 1995

AEO-555

T3
1995
No.58
c.2

ACKNOWLEDGMENTS

I would like to express my appreciation to Dr. Magne Kristiansen for serving as the advisor of my graduate work and chairman of my committee. I would also like to thank the other members of my committee, Dr. E. O'Hair, Dr. L. Hatfield, Dr. T. Trost, and the department representative Dr. D. Merhl for their guidance. I am also grateful to Jim Dickens for his assistance in the design and building of the project.

I would also like to express gratitude to Dr. F. Curran and J. Sankovic. The use of NASA LeRC's research facilities proved invaluable towards the completion of the project. I would also like to thank John Bridges for his assistance in building the hardware.

Finally, I would like to thank my family and especially my girlfriend, Dona, who has provided support and encouragement throughout my academic career.

TABLE OF CONTENTS

ACKNOWLEDGEMENTS ii

LIST OF FIGURES iv

CHAPTER

I. INTRODUCTION 1

II. EXPERIMENTAL SETUP 4

Hall Effect Thrusters 4

Theory of Operation 6

Vacuum Chamber 7

Gas Flow System 8

Power Supply System 9

III. CONTROL SYSTEMS 12

CPU and D/A Board 13

Solid State Relays 13

Isolation Amplifiers 17

Software 20

IV. DATA ACQUISITION 25

DAS16jr A/D Board 25

Compuscope Lite A/D Board 28

Current Probe 29

Langmuir Probe 32

V. CONCLUSIONS 36

REFERENCES 37

LIST OF FIGURES

1. Cutaway view of the TAL 4
2. Cutaway view of the TML 5
3. Cutaway view of the TAL with E and B field directions 7
4. Vacuum chamber with thruster setup 8
5. D-55 and T-100 gas flow system 9
6. SPT-100 gas flow system 9
7. Power supply system for the D-55 10
8. Power supply system for the SPT-100 11
9. Power supply system for the T-100 11
10. Control system of the D-55 thruster 12
11. DDA06 digital-to-analog converter board 13
12. SSR-Rack 24 14
13. Solid state output relay 15
14. SSR MFC circuit 15
15. SSR discharge supply turn on circuit 16
16. AD294 isolation amplifier 17
17. AD294 block diagram 18
18. Isolation amplifier circuit 19
19. Real time configure menu 21
20. Vis Sim main screen 22
21. Discharge supply compound block 23
22. Internal magnet supply compound block 23
23. MFC compound block 24
24. DAS16jr D/A board 25
25. Thruster anode voltage and current measurement setup 26
26. Sensor compound block 27
27. Mass flow measurement setup 27

28. Compuscope Lite A/D board 28
29. Current oscillation measurement setup 29
30. Current oscillations of the D-55 at 300 V and 4.5 A 30
31. Current oscillations of the SPT-100 at 300 V and 4 A 30
32. Current oscillations of the T-100 at 300 V and 4.5 A 31
33. Thruster start up current at 300 V and 4.5 A 32
34. Langmuir probe setup 33
35. General I-V characteristic for a Langmuir probe 33
36. Probe current oscillations 34
37. Probe current during a sweep of the exhaust plume 35

CHAPTER I

INTRODUCTION

The Pulsed Power Laboratory at Texas Tech University is presently investigating the characteristics of several stationary plasma thrusters. In particular, experiments were conducted on the Russian D-55, SPT-100, and T-100 thrusters. With the opening of the Russian market, the US space industry is exploring the feasibility of using these types of thrusters for satellite station-keeping. Performance and evaluation tests of these three thrusters were made at NASA Lewis Research Center in Cleveland, Ohio. In order to perform these tests, a dedicated control and data acquisition system was designed, constructed, and used. This thesis describes these efforts.

In order to investigate these characteristics most efficiently, it was decided to centralize the controls and data acquisition system into a 486 computer. A 6-channel, 12-bit, digital-to-analog converter board with 24 digital input/outputs is dedicated for the control of the thruster. The data acquisition system uses two boards. One is a 16-channel, single ended input, 1 MHz analog-to-digital converter. The other is a 2-channel, high- speed, 20 MHz board. All three boards are integrated using two different software programs, both being Windows compatible.

The plasma thrusters require gas flow and several power supplies for operation. The gas flow is required to deliver Xenon from either one or two feed-throughs, depending on the type of thruster. Up to five different power supplies are needed, including a discharge power supply capable of delivering 10 A at 500 V. The gas flow

and power supplies are all controlled and monitored using the controls computer software.

Controlling the power supplies requires isolation from the D/A board. A hybrid industrial isolation amplifier capable of common mode voltage protection of up to 8 kV is used. Isolation is also required on some of the data acquisition, specifically the discharge voltage and current which are obtained from a simple voltage divider and shunt resistor, respectively.

This thesis details the integration of the data acquisition and control system. The system had three major requirements. The system hardware was assembled at Texas Tech University while the actual experiment was done at NASA Lewis Research Center in Cleveland, Ohio, therefore, the system had to be portable. Also, at the beginning of the project, the actual characteristics of the thruster to be examined were yet to be determined, therefore, the system had to be flexible. Finally, being able to run three different thrusters required the system to be generic.

The thruster characteristic studied was plume fluctuations, specifically, plasma oscillations. Diagnostics used to measure the plasma oscillations are a current sensor and a Langmuir probe. The current sensor was used to measure the oscillations of the discharge current. The Langmuir probe was used to detect the oscillations of the electron density. Both were recorded using the 20 MHz A/D board.

Chapter II of this thesis describes the experimental setup of the project which includes a description of the thrusters and the hardware required to operate them. Chapter III explains the control system including the D/A board, isolation system, and

software. Chapter IV details the data acquisition system which includes A/D boards, measurement setup, and software. Finally, Chapter VI entails the conclusions.

CHAPTER II

EXPERIMENTAL SETUP

Hall Effect Thrusters

The first Hall Effect thruster tested was the D-55 stationary plasma thruster with anode layer (TAL) (Figure 1), manufactured by the Central Scientific Research Institute of Machine Building (TsNIIMASH) in Russia. Anode layer refers to the fact that the ionization and acceleration regions are near the anode. The 55 refers to the diameter in millimeters of the anode. There are two magnets, an external and an internal, each with a dedicated power supply. The Xenon feed has two different lines, one to the cathode and

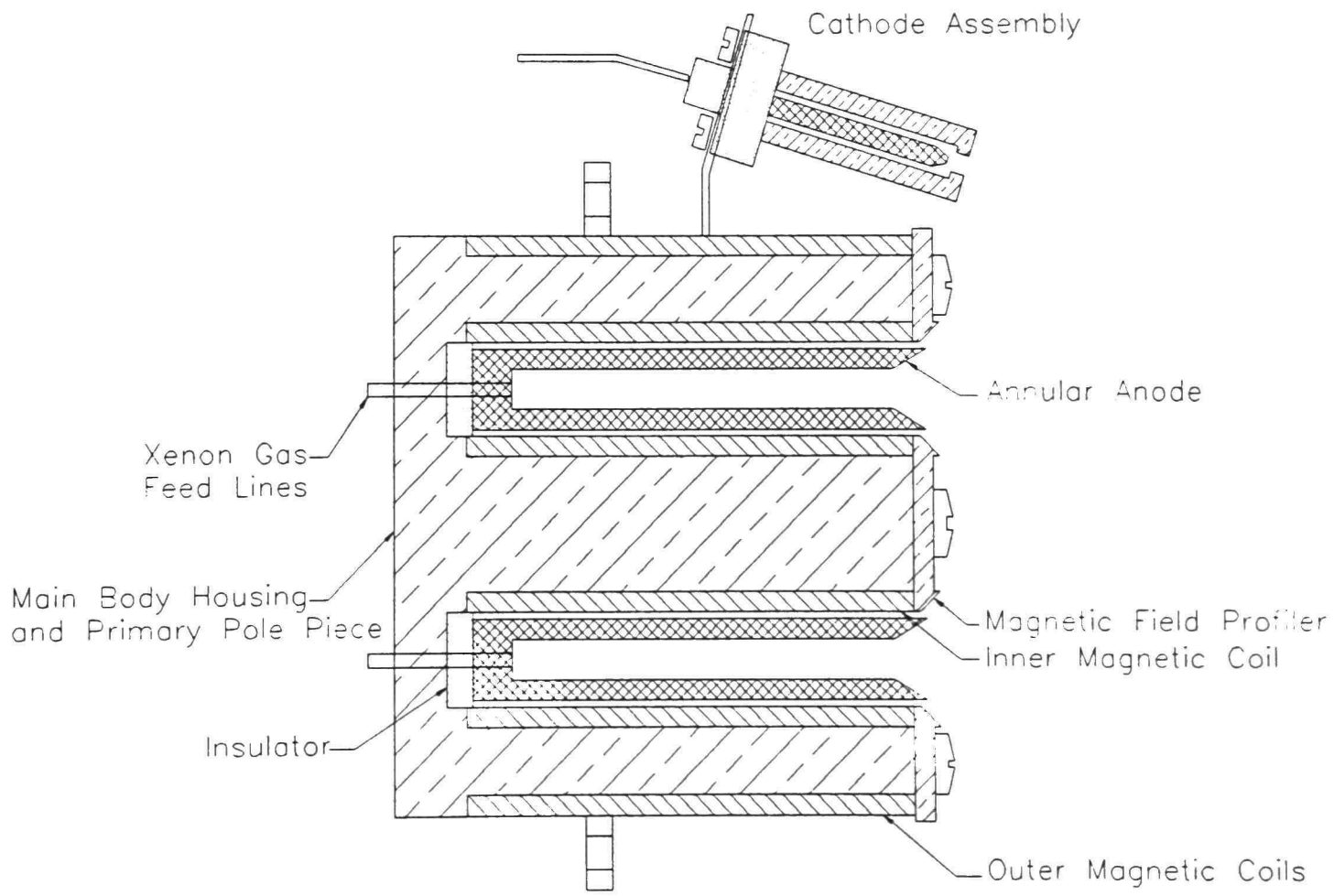

Figure 1 - Cutaway view of the TAL

the other to the anode. The Xenon anode feed at the thruster is evenly spaced so as to uniformly distribute the gas flow. The thruster is designed with a hollow cathode assembly consisting of an emitter, heater coil, and keeper.[1]

The second Hall Effect thruster tested was the SPT-100 stationary plasma thruster with magnetic layer, shown in Figure 2, designed and built by Fakel Enterprises, also in Russia. Thruster with magnetic layer (TML), refers to the fact that the acceleration region is away from the anode in the magnetic layer, unlike the TAL. The 100 refers to the length in millimeters of the acceleration region. There is one Xenon feed line which splits between the anode and cathode internally, with a 92%/8% ratio, respectively. The magnet system consists of one internal and 4 external electromagnets, all powered by the discharge power supply. The thruster is equipped with two cathode assemblies for redundancy. Each cathode consists of an emitter, heater coil, thermal screens, and igniter, similar to the D-55.

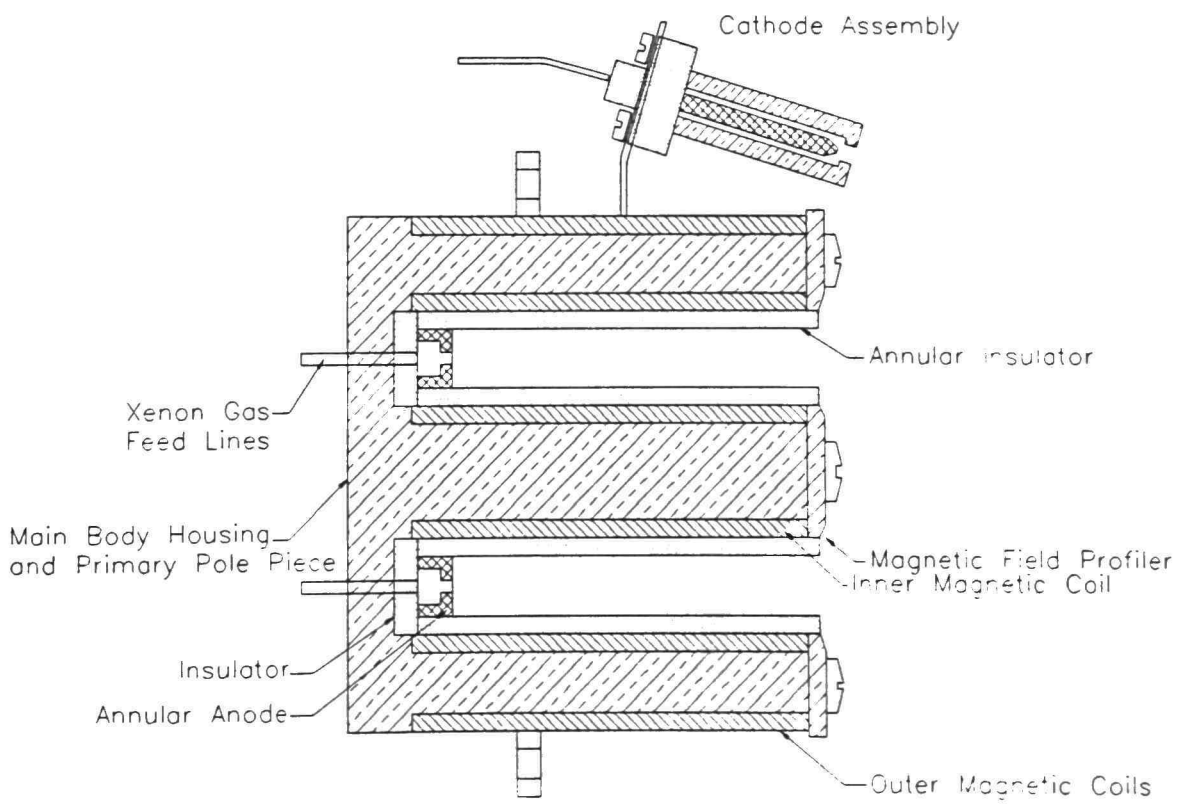

Figure 2 - Cutaway view of the TML

The Hall Effect thruster tested was the T-100 manufactured by the Institute of Thermal Processes (NIITP) in Russia. The T-100 is similar to the SPT-100 in that it is a TML. However, like the D-55, its internal and external electromagnets require dedicated power supplies and the Xenon flow to the cathode and anode are controlled separately.

Theory of Operation[2]

The general theory of operation of the Hall Effect thruster is similar for both the TML and TAL concepts. At startup, electrons are emitted from the cathode by heating the flow of Xenon and by applying a high voltage, around 2 kV, to the igniter. A voltage is then applied to the anode and the magnets. The electrons emitted from the neutralizer are attracted to the anode by the established E field. When the electrons initially enter the magnetic field, they experience a force described by:

$$\vec{F} = Q(\vec{U} \times \vec{B})$$

where Q is the electron charge, $\vec{U}$ is the electron velocity, and $\vec{B}$ is the magnetic flux density. The electrons are then caught in this magnetic field moving in a cyclotron motion and forming a virtual cathode at the end of the anode chamber. A diagram of the TAL with E and B field directions is shown in Figure 3.

Xenon atoms diffuse down the anode chamber until they collide with the circulating electrons. These collisions produce Xenon ions which are attracted to the virtual cathode at the end of the chamber. The Xenon ions are then propelled out the end of the chamber.

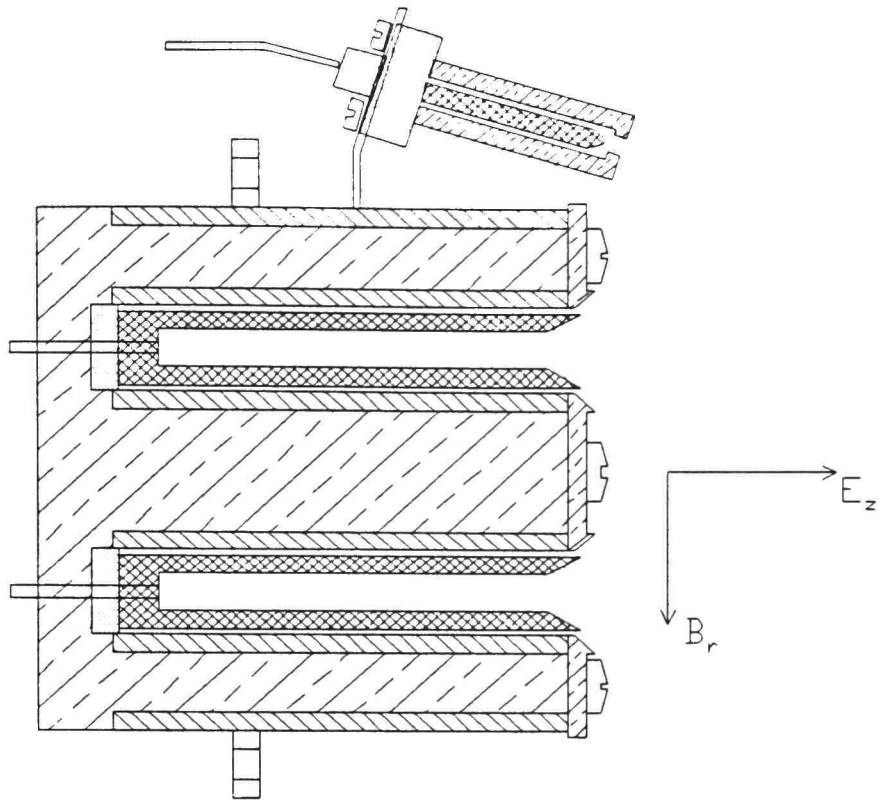

Figure 3 - Cutaway of the TAL with E and B field directions

The Xenon ions are accelerated by the electric field to velocities of about 16,000 m/s. Electrons from the cathode serve to neutralize the ion beam. Due to the relatively large mass of the Xenon ions, they are largely unaffected by the magnetic field. However, some bending of the ion trajectories occurs and results in a small torque about the z-axis.

Vacuum Chamber

The experiments were performed at NASA Lewis Research Center at Cleveland, Ohio, in tanks 3 and 8. The vacuum facilities of each are very similar. Each work off of four 32" diffusion pumps. Each have roughly the same dimensions, 1.5 m inside diameter by 4 m long. Refer to Figure 4 for a schematic diagram. The base pressure of each tank was approximately 10^{-6} torr with an operating pressure of $5 \cdot 10^{-5}$ torr which is

$5 \cdot 10^{-5}$ torr which is well below the $2 \cdot 10^{-4}$ torr operating pressure suggested by the thruster's manufacturers.

The thruster is located at the end of the vacuum chamber. A cylindrical Langmuir probe is mounted inside the chamber in the middle of the exhaust plume and at a certain distance from the exit plane.

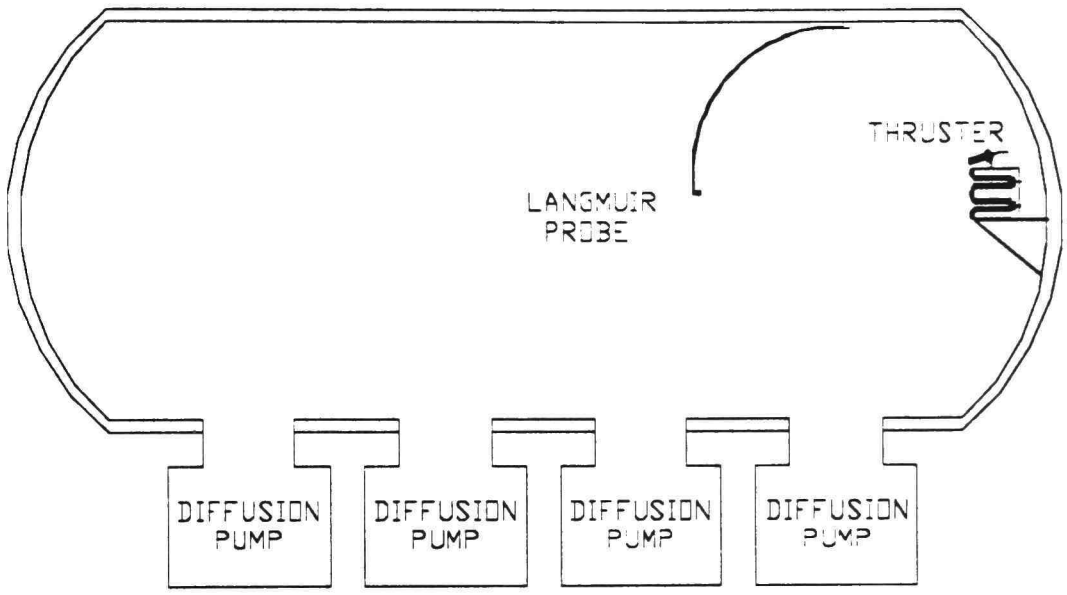

Figure 4 - Vacuum chamber with thruster setup

Gas Flow System

The propellant system is supplied with 99.99% pure Xenon. A schematic diagram of the propellant system for the D-55 and T-100 is shown in Figure 5. Three manual valves are used, one main valve and one valve on each branch. The mass flow for the cathode branch is controlled using a 20 standard cubic centimeter (sccm), mass flow controller (mfc). The anode is controlled with a 100 sccm mfc. The conversion of units from sccm to milligram/second, (mg/s), for Xenon is:

$$1 \text{ sccm} \approx 0.1 \text{ mg} / \text{s}.$$

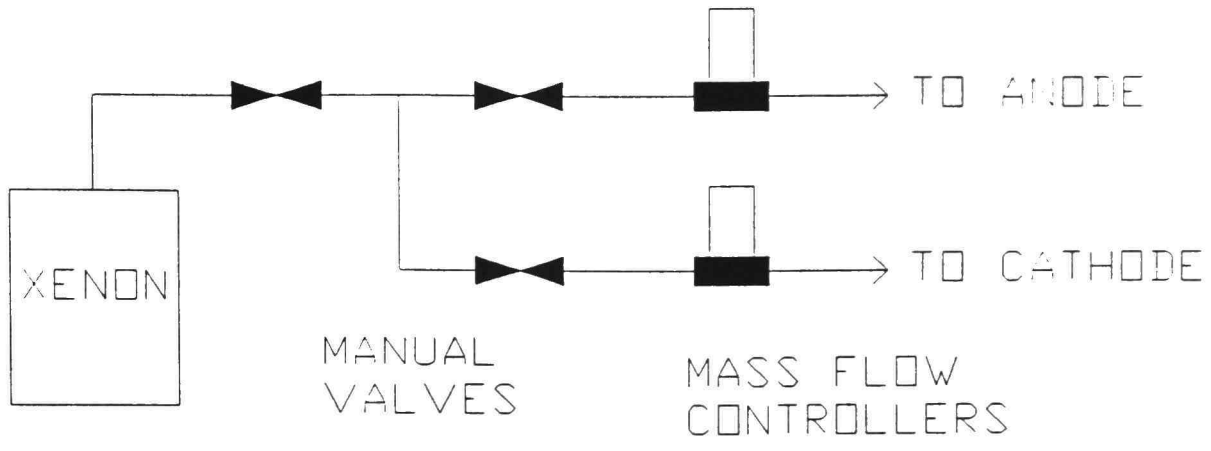

Figure 5 - D-55 and T-100 gas flow system

The mfc's are controlled with a power supply controller. The channels are operated in automatic mode and controlled using the D/A converter board. Both the mfc's and power supply are manufactured by Units Instruments Inc.

As mentioned before, Figure 5 shows the gas supply setup for the D-55 and T-100. The SPT 100, however, requires only one gas feed since the flow to the anode and cathode is split internally. As a result, only one branch is used; see Figure 6.

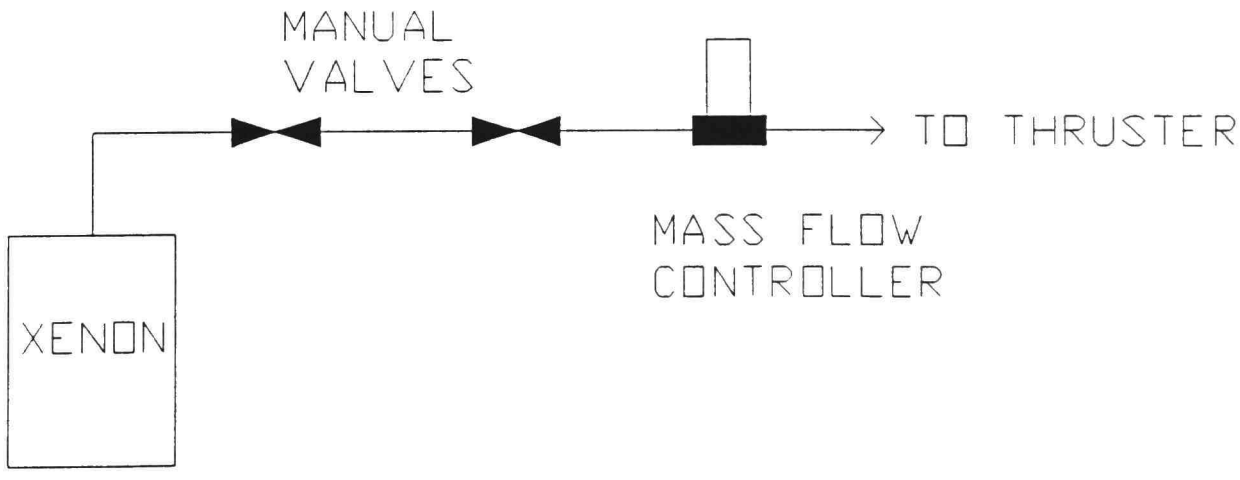

Figure 6 - SPT-100 gas flow system

Power Supply System

The thruster discharge current is supplied by a 5 kW switching power supply manufactured by Electronic Measurements. The supply is capable of delivering 10 A at

500 V, which meets the requirements of all the thrusters tested. The cathode heater, external magnet, and internal magnet currents are supplied by dedicated 360 W power supplies manufactured by Kikusui. The supplies are capable of delivering 12 A at 30 V. A 3 kW switching power supply, manufactured by Electronics Measurements, is used for the igniter. This supply is capable of delivering 5 A at 600 V. Figure 7 shows the setup of the power supply system for the D-55. There is a 10 Ω ballast resistor and a 100 μ F capacitor to attenuate the current oscillations caused by the thruster.

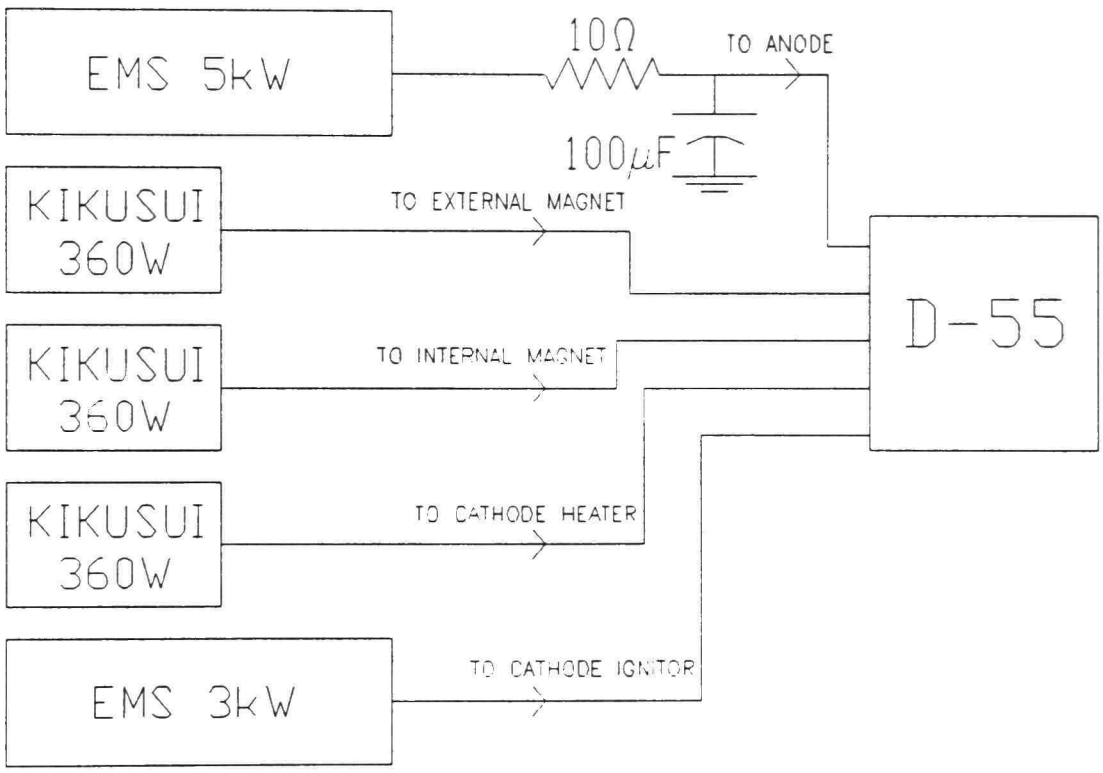

Figure 7 - Power supply system for the D-55

The SPT-100 setup, shown in Figure 8, is slightly different than the D-55. Only three power supplies are used as opposed to five used on the D-55. The magnet coils are powered by the discharge supply. Consequently, the magnetic field cannot be controlled independently from the electric field.

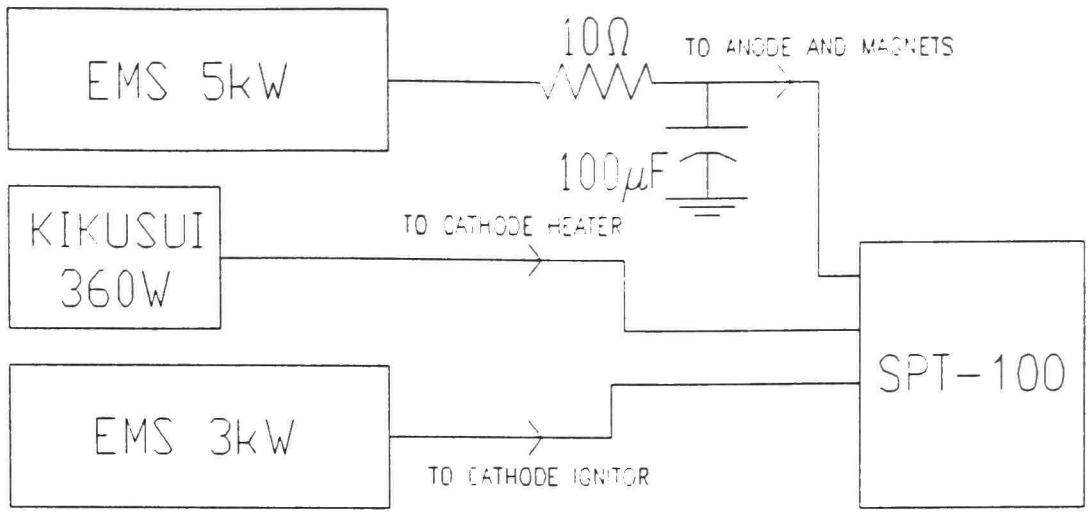

Figure 8 - Power supply system for the SPT-100

The T-100 setup, shown in Figure 9, is very similar to the D-55 with the only difference being the absence of the cathode heater.

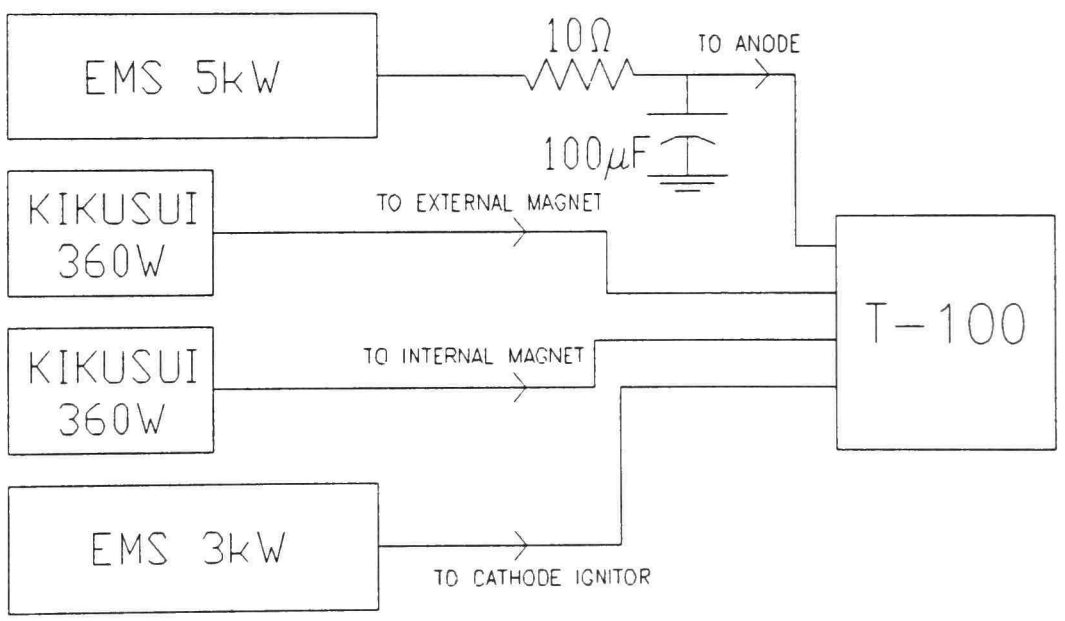

Figure 9 - Power supply system for the T-100

CHAPTER III

CONTROL SYSTEMS

The major requirement of the control system is to control remotely the gas flow and power to the thruster from a central location. This is most easily achieved by integrating a personal computer, a digital-to-analog board, control software, isolation amplifiers, and solid state relays. Figure 10 shows the overall view of the control system for the D-55. Notice that the EMS 3 kW power supply is not contained in the control system. This is for two reasons. First, this supply is dedicated for the cathode igniter which is only used during initial startup and is then immediately shut off. Second, the control of this supply would require one more D/A channel than was available from the board used.

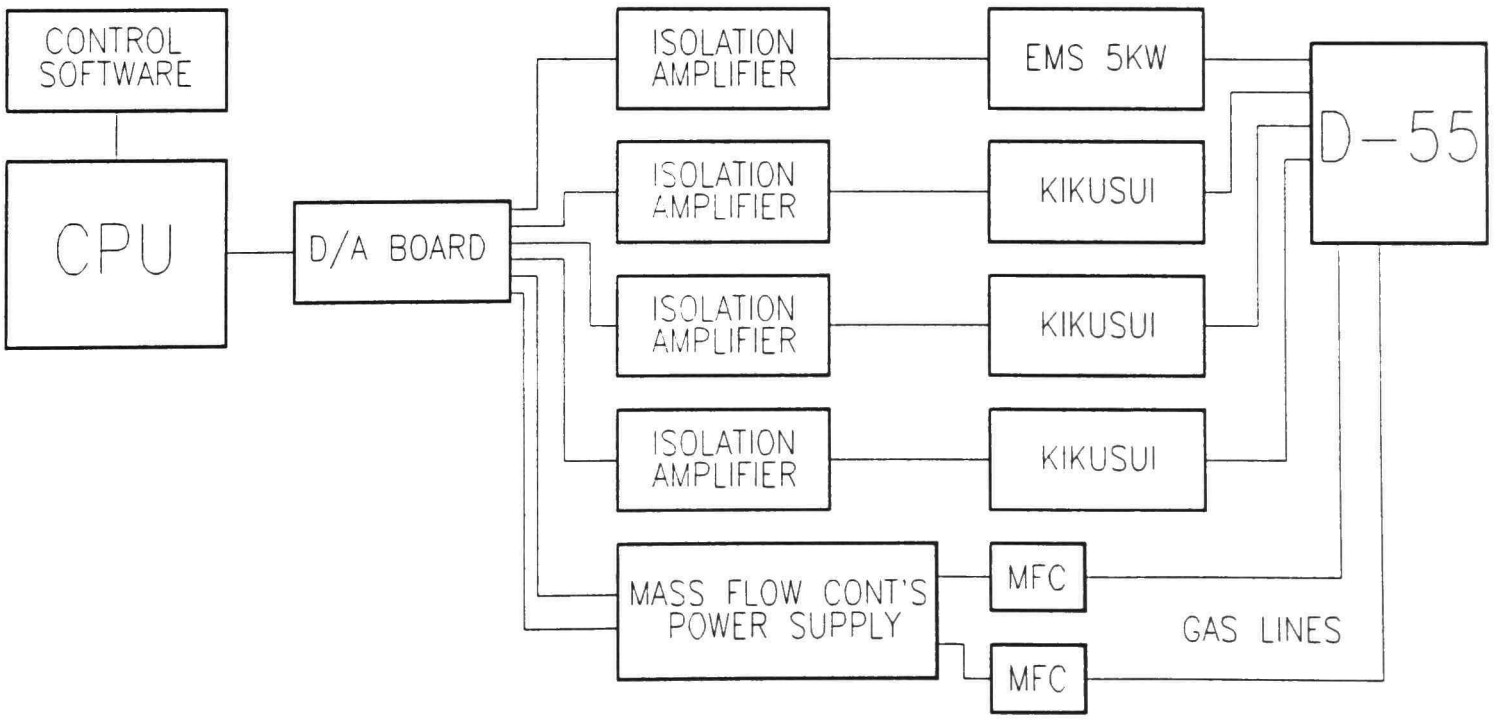

Figure 10 - Control system of the D-55 thruster

CPU and D/A Board

The PC is a 486 50 MHz IBM clone with 8 Mbytes of RAM. The D/A board is the CIO-DDA06/12 made by Computer Boards, Inc. The DDA06, shown in Figure 11, is actually two boards in one.[3] It is equipped with 24-bit digital input/outputs and 6 analog output channels with 12 bit (1 part in 4,095) resolution.

The analog output range is fully switch selectable from 0-1.67 to 0-5 V in unipolar mode and +/-1.67 to +/-10 V in bipolar mode. The range selected for this application is 0-5 V unipolar which gives 1.22 mV/bit resolution. The digital output range is 2.4 V minimum for output high and 0.5 V maximum for output low.

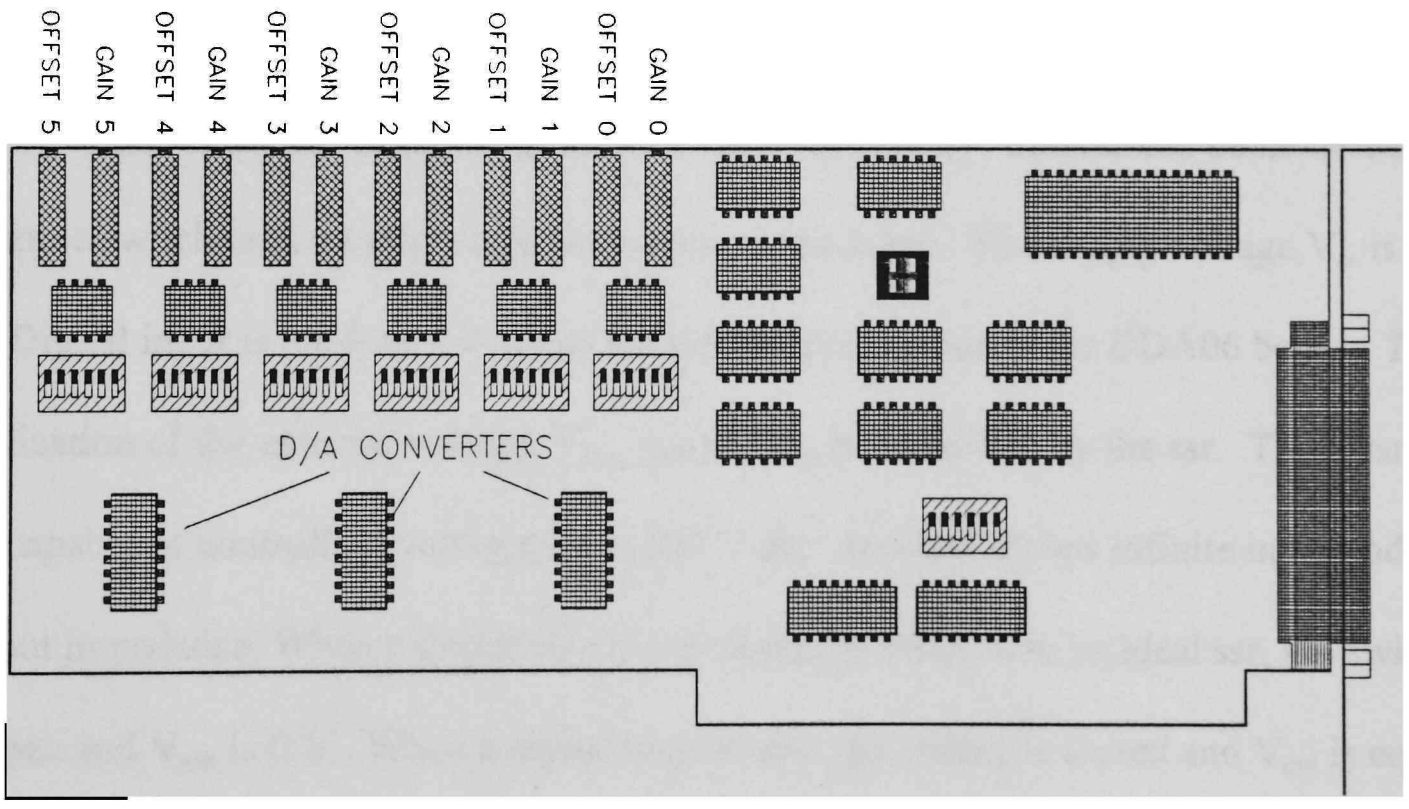

Figure 11 - The DDA06 digital-to-analog converter board

Solid State Relays

The digital input/outputs work in conjunction with solid state relays to provide over 4 kV isolation and allow the DDA06 to sense or control high AC and DC voltages.

The solid state relays (ssr) mount on the SSR-RACK 24, shown in Figure 12, and interface directly to the DDA06.

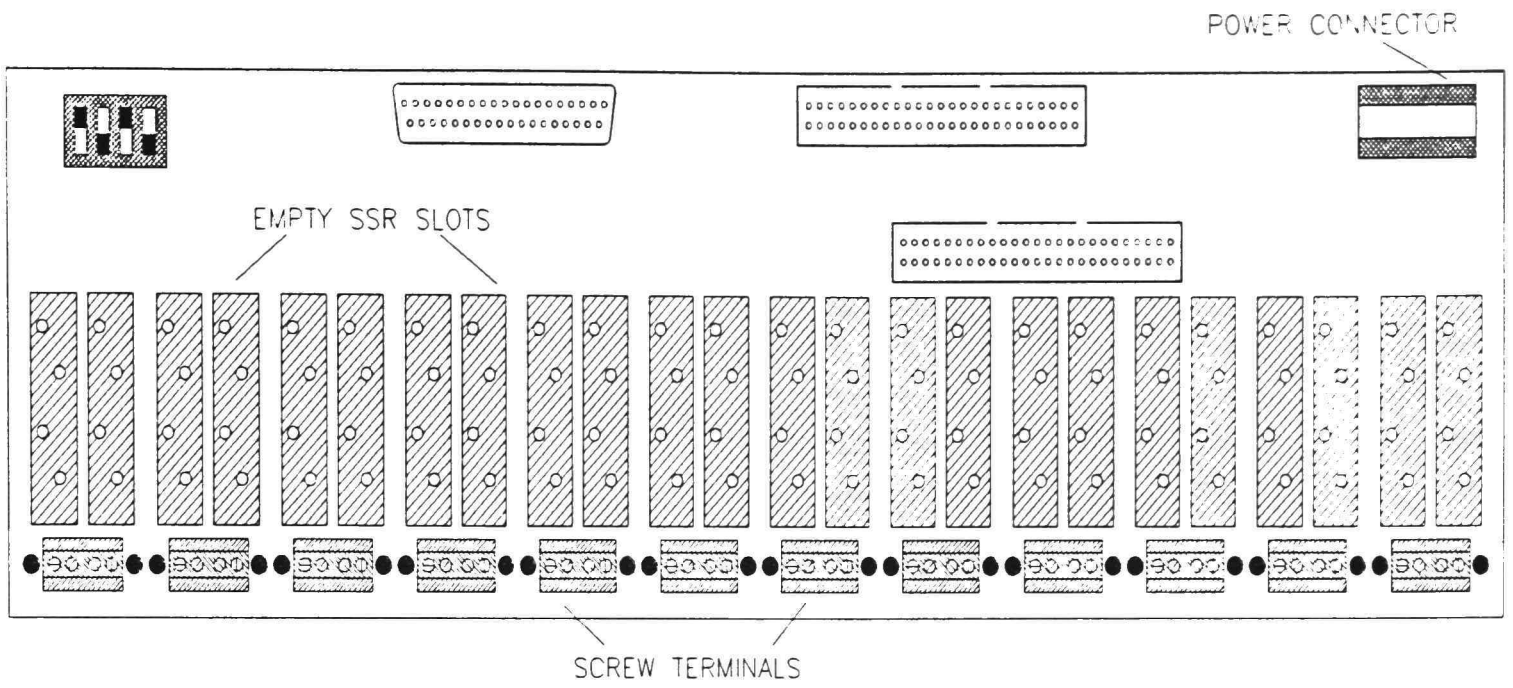

Figure 12 - SSR-Rack 24

Figure 13 shows a model of a typical solid state relay. The ssr can be modeled as a simple switch with a certain input and output impedance. The supply voltage, V_s, is 5 V. Digital input is the 0 or 5 V signal from the digital output of the DDA06 board. The application of the external voltage, V_{ext}, across V_{out} is controlled by the ssr. These ssr's are capable of controlling voltages up to 600 V dc. An ideal ssr has infinite input and output impedance. When a digital low is sent from the DDA06 to an ideal ssr, the switch is open and V_{out} is 0 V. When a digital high is sent, the switch is closed and V_{out} is equal to V_{ext}. Realistically, values for R_{in} and R_{out} are approximately 1 MΩ and 40 kΩ, respectively.

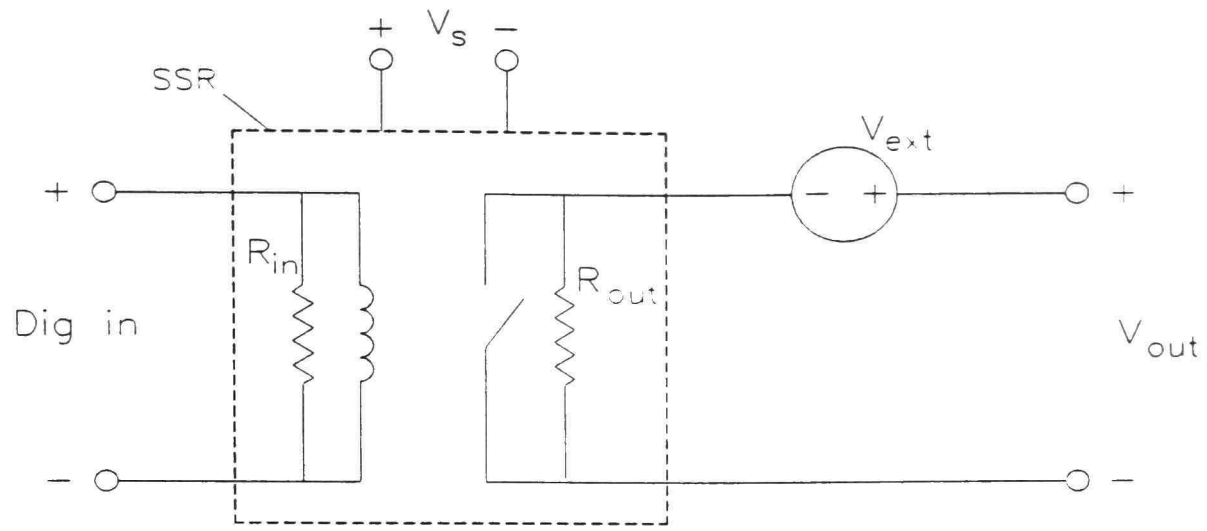

Figure 13 - Solid state output relay

One application of the ssr's is the remote turn-on of the mass flow controllers (mfc), shown in Figure 14. The control turn on voltage, Vin, for the mfc's on the power

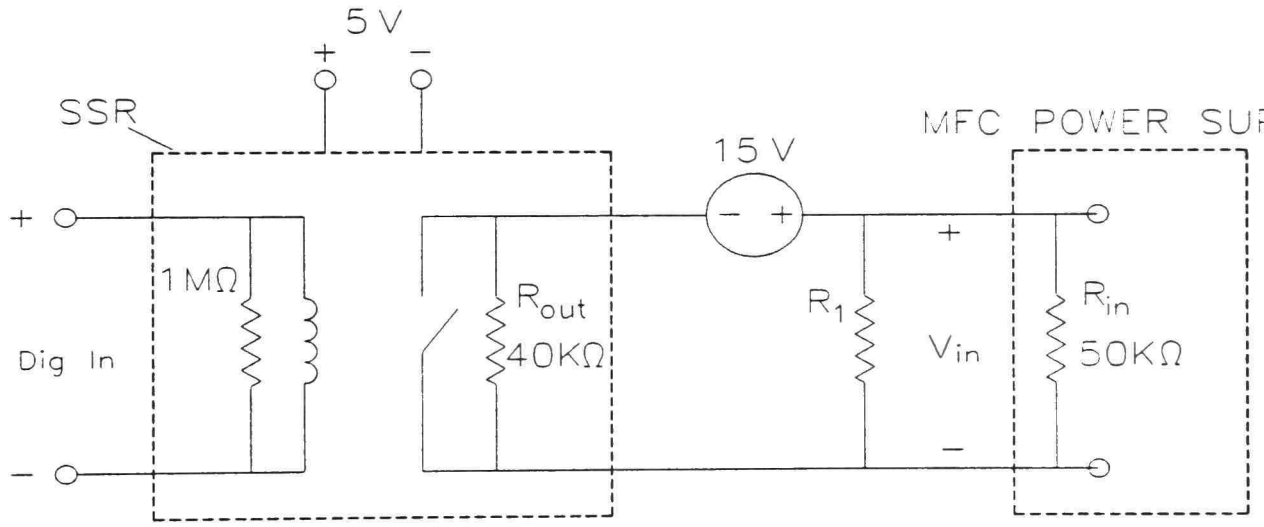

Figure 14 - SSR MFC circuit

supply is asserted low. A V_{in} of 0 to 7.5 V turns on the mfc while a V_{in} of 7.5 to 15 V turns off the mfc. With the switch closed, there is 15 V across R_{in} so that the mfc is turned off since it is asserted low. When the switch is opened, a voltage of less than 7.5 V is desired in order to turn on the mfc. Consider first $R_1 = 0\,\Omega$ in the circuit of Figure 14. When the switch is opened, V_{in} changes from 15 V in the ideal case to:

$$\text{Vin} = 15\frac{\text{Rin}}{\text{Rin} + \text{Rout}} = 15\frac{50\ \text{k}\Omega}{50\ \text{k}\Omega + 40\ \text{k}\Omega} = 8.33\ \text{V}.$$

This is inadequate. Therefore, a resistor R_1 is placed in parallel with R_{in} to lower the mfc input impedance. If R_1 is chosen to be 1 kΩ:

$$Vin = 15\frac{Rin \| R1}{Rin \| R1 + Rout} = 15\frac{980\ \Omega}{980\ \Omega + 40\ k\Omega} = 0.359\ V.$$

This V_{in} is much more desirable.

The other application of the ssr's is the remote turn-on of the 5 kW EMS discharge power supply. This is done by applying a dry contactor switch between two of the program terminals. The circuit required, shown in Figure 15, is a slightly more complex circuit than the relay mfc circuit.

Consider first the ssr switch open in the circuit of Figure 15. The V_{in} at the dry contact switch input terminals is approximately 7.2 V. The dry contact switch requires 12 V to close. Therefore, the dry contact switch is open and the EMS power supply is off.

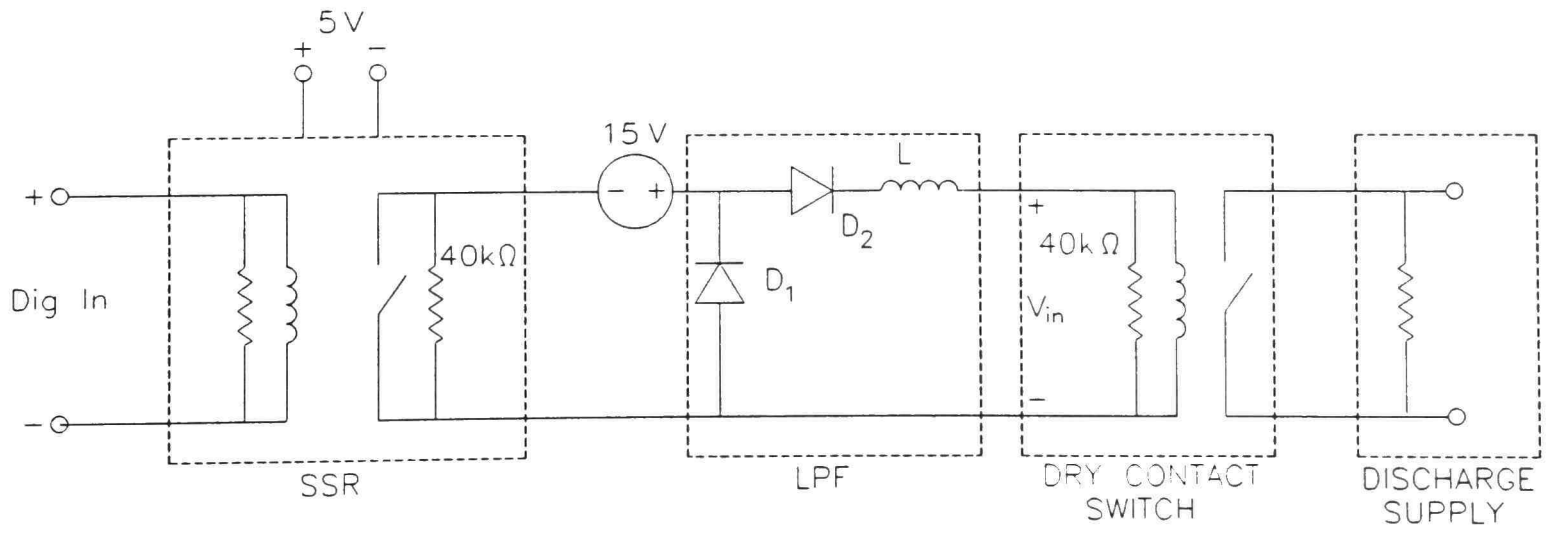

Figure 15 - SSR discharge supply turn-on circuit

Next, consider what happens when the ssr switch is closed. The V_{in} at the dry contact switch input terminals is 14.3 V. This closes the dry contact switch and the EMS

5 kW supply is turned on. Unfortunately, the Kikusui and EMS 3 kW supplies did not have remote turn on capability. Therefore, the circuit in Figure 15 was used only with the EMS 5 kW supply.

Isolation Amplifiers

The EMS and Kikusui power supplies are equipped with an external voltage control capability. An externally applied voltage from 0 to 5 V will vary the output of the individual power supplies from 0 to full rated voltage or current. However, the applied voltage is required to be isolated. This is achieved by the use of an isolation amplifier. The type used is an Analog Devices AD294A isolation amplifier,[4] shown in Figure 16, capable of common-mode voltage protection of +/-8 kV and a frequency response of

-3dB from 0 to 2.5 kHz.

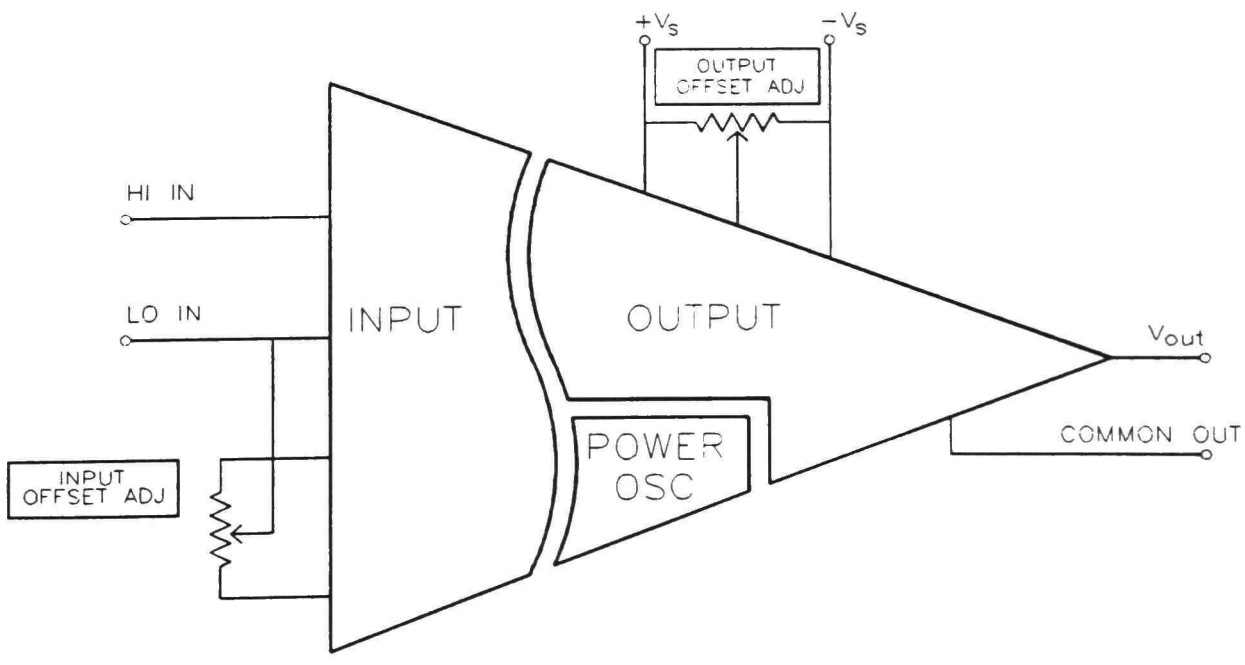

Figure 16 - The AD294 isolation amplifier

The AD294's performance is attributed to the use of a hybrid magnetic ceramic transformer, T1, shown in Figure 17. Windings are screened on two ceramic alumina substrates which are placed together separated by a ceramic isolation barrier. Both power and signals are transferred between the amplifier's input stage and output via T1. The input signal is filtered and appears at the input of the inverting amplifier, A1. The gain of A1 is set by placing a resistor between R_G and COM_{IN}.

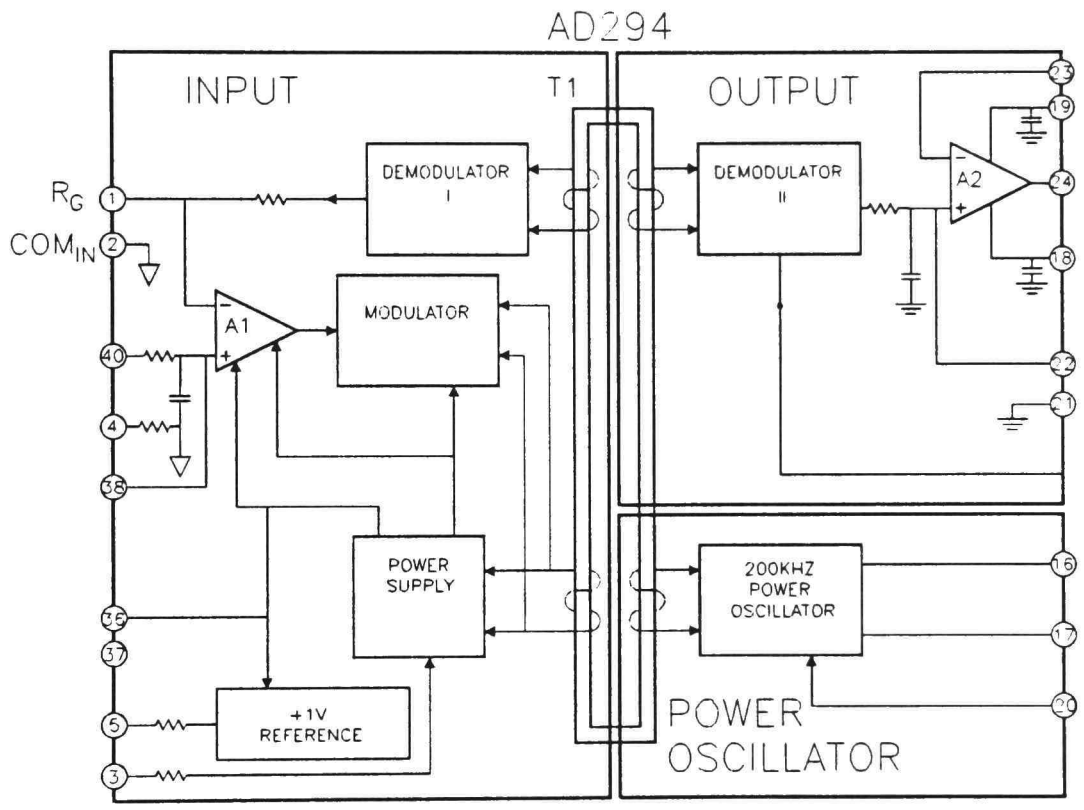

Figure 17 - AD294 block diagram

For this application the input and output gains are both set to 1. The output of A1 is modulated, carried across the isolation barrier by signal transformer, T1, and demodulated. The demodulated output voltage is filtered and then buffered by A2. The 200 kHz square-wave power oscillator drives the primary windings of transformer, T1. The secondary windings of T1 then energizes the input power supply and drives both the modulator and demodulator.

A total of 8 isolation amplifier circuits were used for this experiment. Two printed circuit boards were built, both with 4 isolation amplifier circuits. Each circuit consists of an isolation amplifier and a +/-15 V power supply. A dedicated power supply for each isolation amplifier was required to provide isolation of one amplifier from the others. A circuit for one of the isolation amplifiers is shown in Figure 18.

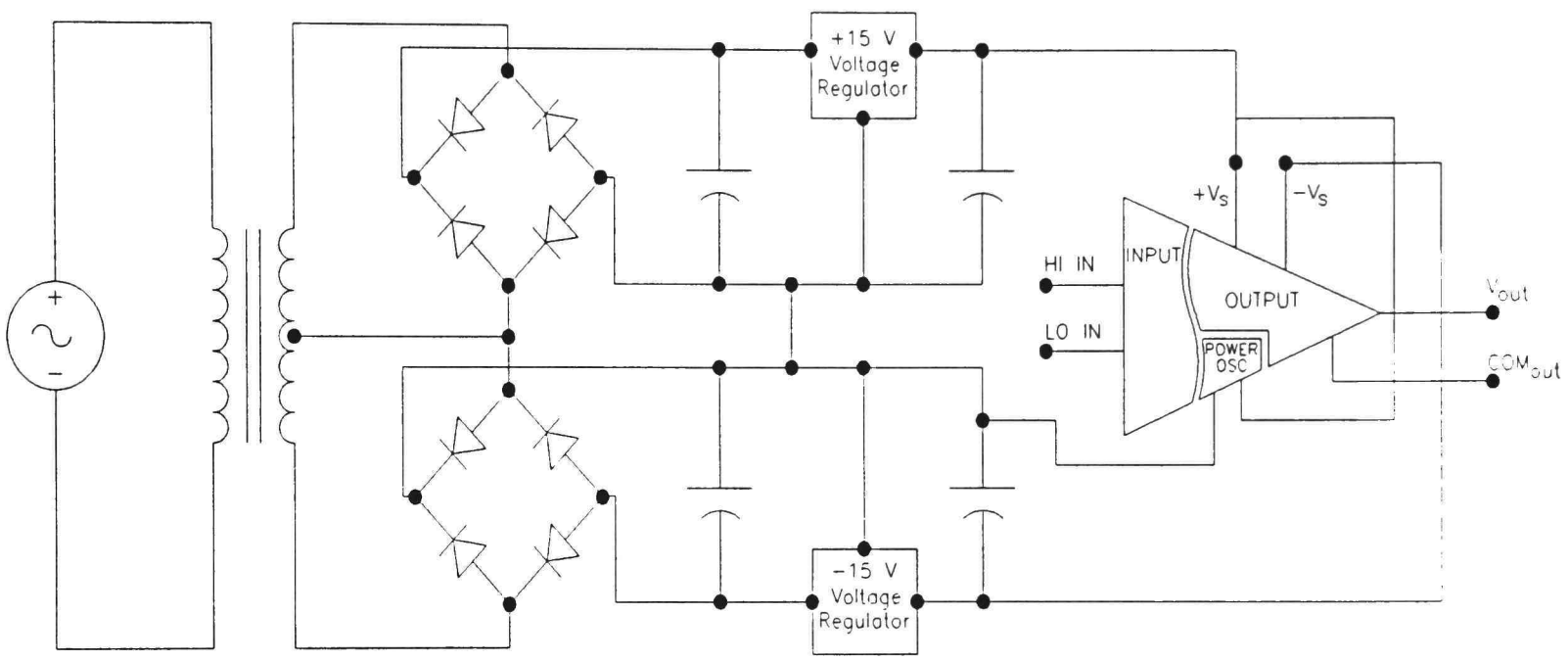

Figure 18 - Isolation Amplifier Circuit

The boards were mounted inside a rack-mountable aluminum chassis. Banana and DB ribbon cable connectors were mounted on the exterior of the chassis for inputs and outputs to and from the isolation boards.

One of the isolation boards is dedicated for use with the DDA06 analog outputs. Channel 0, 3, 4, and 5 outputs are connected to the inputs of the isolation amplifiers. The outputs of these isolation amplifiers are connected to the external voltage controls of the 5kW EMS and the three Kikusui power supplies. The other isolation board is used for data acquisition and will be discussed in the next chapter.

Software

By using the isolation amplifiers, solid state relays, CPU, and DDA06 digital-to-analog board it is possible to control the operation of a Hall thruster remotely. All these devices are integrated with a real time controls software program. The specific program used is Vis Sim/RT and Vis Sim/DACQ created by Visual Solutions.[5] Vis Sim/RT makes it possible to send and receive data from digital-to-analog and analog-to-digital boards, respectively. The Vis Sim/DACQ program links Vis Sim with Vis Sim/RT. Vis Sim is a controls simulation program which uses a block diagram programming method. Vis Sim has block subroutines such as integrators, differentiators, and Fourier transforms as well as many others. Under Vis Sim/DACQ, block diagrams are limited to 100 blocks.

The Vis Sim real-time drivers consist of two parts, a real-mode Terminational Stay Resident (TSR) interrupt handler that is installed from the MS/DOS prompt, and a Vis Sim Dynamic Link Library (DLL) file that provides an MS/Windows protected mode interface to the DOS TSR. The command to load the DOS TSR for the DDA06 board is:

DAS8.EXE -dDDA06=300 -dPIO24=30A -i6A.

DAS8.EXE is the TSR file name. -dDDA06 accesses the D/A outputs of the DDA06 and sets the hexadecimal address at 300. -dPIO24 accesses the digital I/O of the DDA06 and sets 30A as its hexadecimal address. This is done because the DDA06 is comprised of separate D/A channels and digital I/O. Finally, -16A is the TSR interrupt address.

Once the drivers are loaded, the boards need to be made compatible with the software. This is done by using the file menu Real Time Configure menu, shown in Figure 19, from within Vis Sim. The DDA06 is actually configured as two boards. One is used to access the D/A channels and the other to access the digital I/O.

Once all the boards are configured, the simulation program can be written. As mentioned earlier, Vis Sim is a block diagram programming package. From the main screen, shown in Figure 20, the user is able to control fully the routine operation of the Hall thrusters. The slider blocks control the analog outputs of the DDA06. Varying the

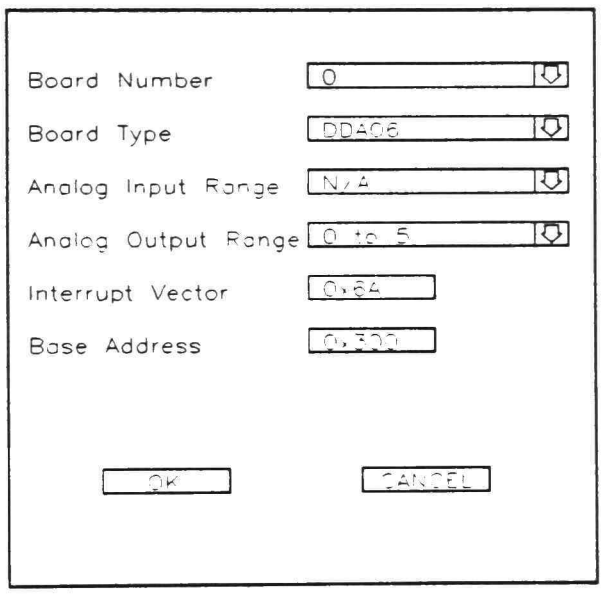

Figure 19 - Real time configure menu

slider from its minimum to maximum values will vary the analog output channel from 0 to 5 volts, respectively. The minimum and maximum values of the slider are chosen to represent the minimum and maximum values of the equipment that the slider is controlling. For example, the voltage range of the 5kW EMS power supply is 0 to 600 volts which can be controlled with a 0 to 5 volt external voltage. The slider ranges from 0 to 600, and its output is multiplied with a gain of .00833 (see Figure 21). So, the input to the DDA06 analog output is 0 to 5 volts.

The button blocks labeled "equipment on" act as on/off switches. The on/off buttons for the discharge supply and the two mfc's control the solid state relays. However, since the Kikusui supplies are not equipped for remote turn on, the buttons are not used to control ssr's. Instead, the buttons turn on and off the voltage from the analog outputs.

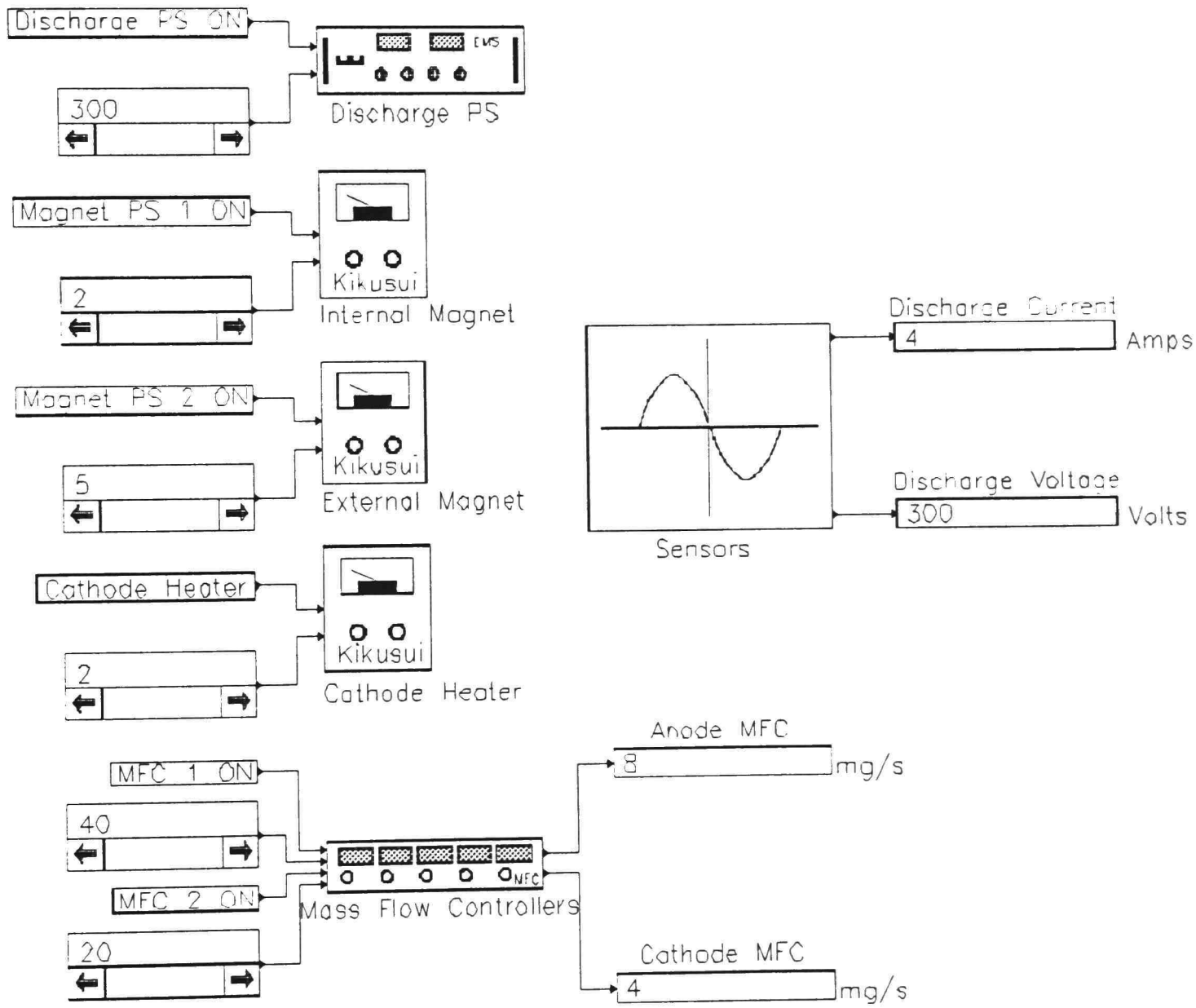

Figure 20 - Vis Sim main screen

The equipment blocks, i.e., discharge PS and mass flow controllers, are actually compound blocks. That is, they contain a group of blocks. Figure 21 displays the compound block of the discharge power supply. Note that the outputs from the button

and slider enter the compound from the left. As mentioned earlier, the output of the slider gets multiplied by a 0.00833 gain, and is then sent to analog output channel 1 of the DDA06.

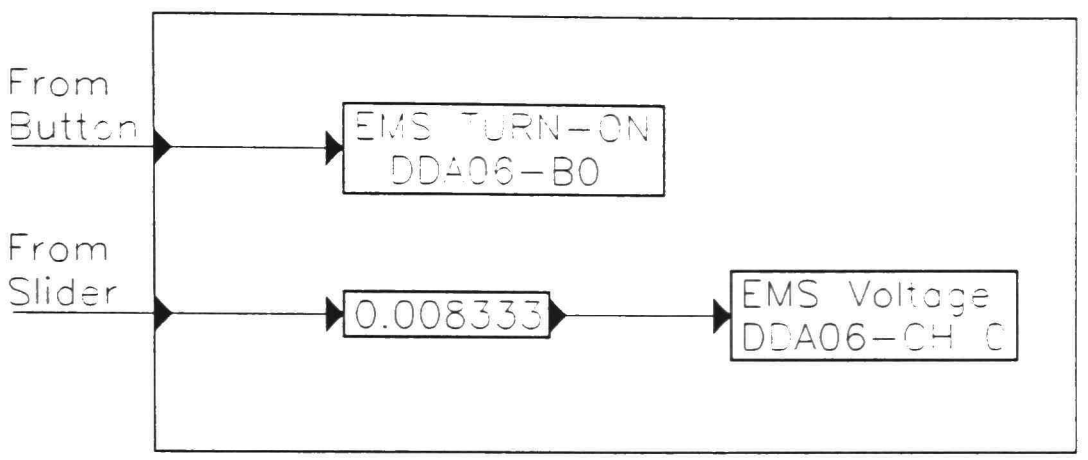

Figure 21 - Discharge supply compound block

The output of the buttons is sent directly to digital output channel B0. When the button is in the on mode, a digital high is sent by channel B0 to the SSR. This closes the dry contact switch and turns the discharge power supply "on".

The internal magnet compound block is shown in Figure 22. Notice that the output of the button is multiplied with the slider. When the button output is 0 there is no voltage sent from the DDA06 channel 3. When the button output is 1, the DDA06 channel 3 output is determined by the slider. The external magnet and heater compound blocks have the same setup as the internal magnet block.

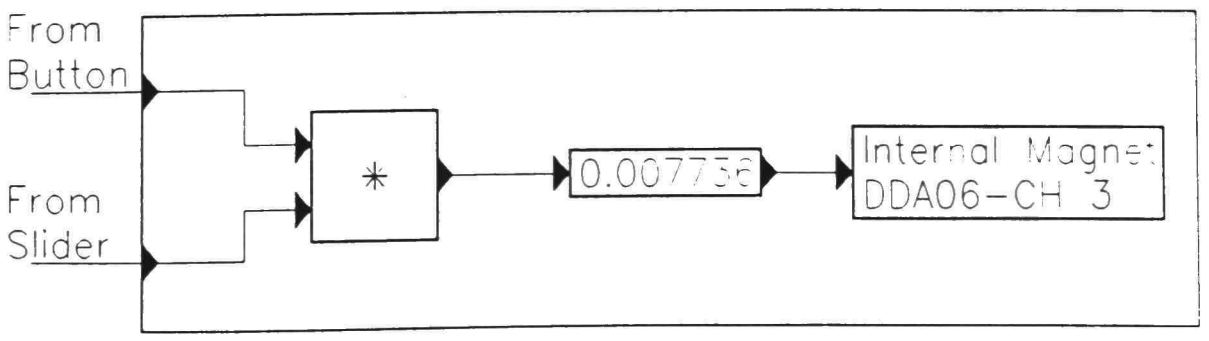

Figure 22 - Internal magnet supply compound block

The mass flow controller compound block is shown in Figure 23. The button output goes through a not gate and then to the digital output. Remember that the mass flow controller enables are asserted low. So, in order to stay consistent with the discharge supply on/off button, a not gate is used. The slider control controls the set point of each respective mfc. Blocks labeled DAS16jr are used for reading the actual flow of Xenon through each mfc. These will be discussed in the next chapter.

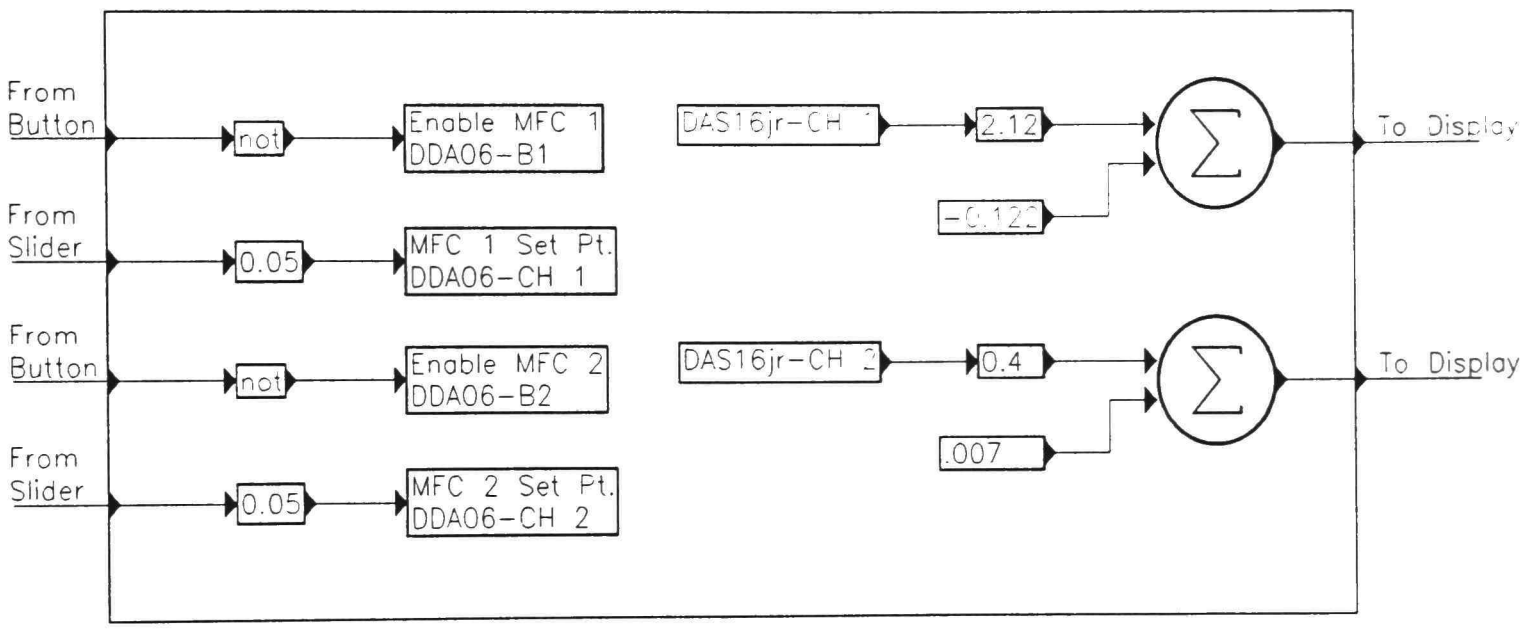

Figure 23 - MFC compound block

CHAPTER IV

DATA ACQUISITION

Data Acquisition for this project is broken up into two parts. First, a DAS16jr analog-to-digital (A/D) board is used for the slow-speed monitoring of Xenon gas flow and thruster anode voltage and current. Second, a 20 MHz Compuscope Lite A/D board is used for the high-speed monitoring of thruster current oscillations and Langmuir probe current.

DAS16jr A/D Board

The DAS16jr,[6] shown in Figure 24, is a 1 MHz A/D board. It has 16 channels in single ended mode and 8 channels in differential input mode. The input range is programmable with a default mode of 0 to 5 V.

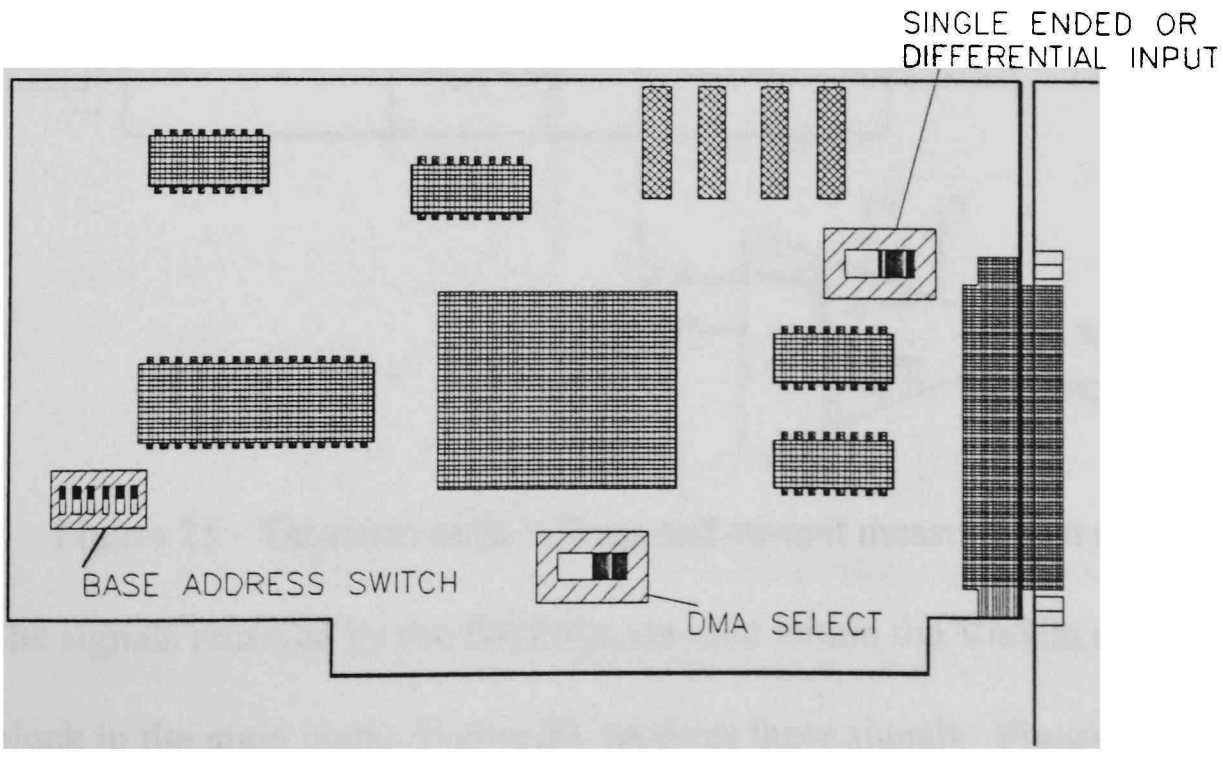

Figure 24 - DAS16jr D/A board

One of the uses of the DAS16jr board is monitoring of the thruster during operation. This includes parameters such as anode voltage, anode current, and Xenon gas flow. Anode voltage and current are monitored by use of a voltage divider and shunt resistor, respectively. The setup is displayed in Figure 25. Typical values for anode voltage and current are 300 V and 5 A. For an anode voltage of 300 V, the voltage across the 100 Ω resistor is approximately 3 V. Similarly, for an anode current of 5 A, the voltage across the 0.5 Ω resistor is 2.5 V. The output of each of these resistors are sent through an isolation amplifier and then to the DAS16jr.

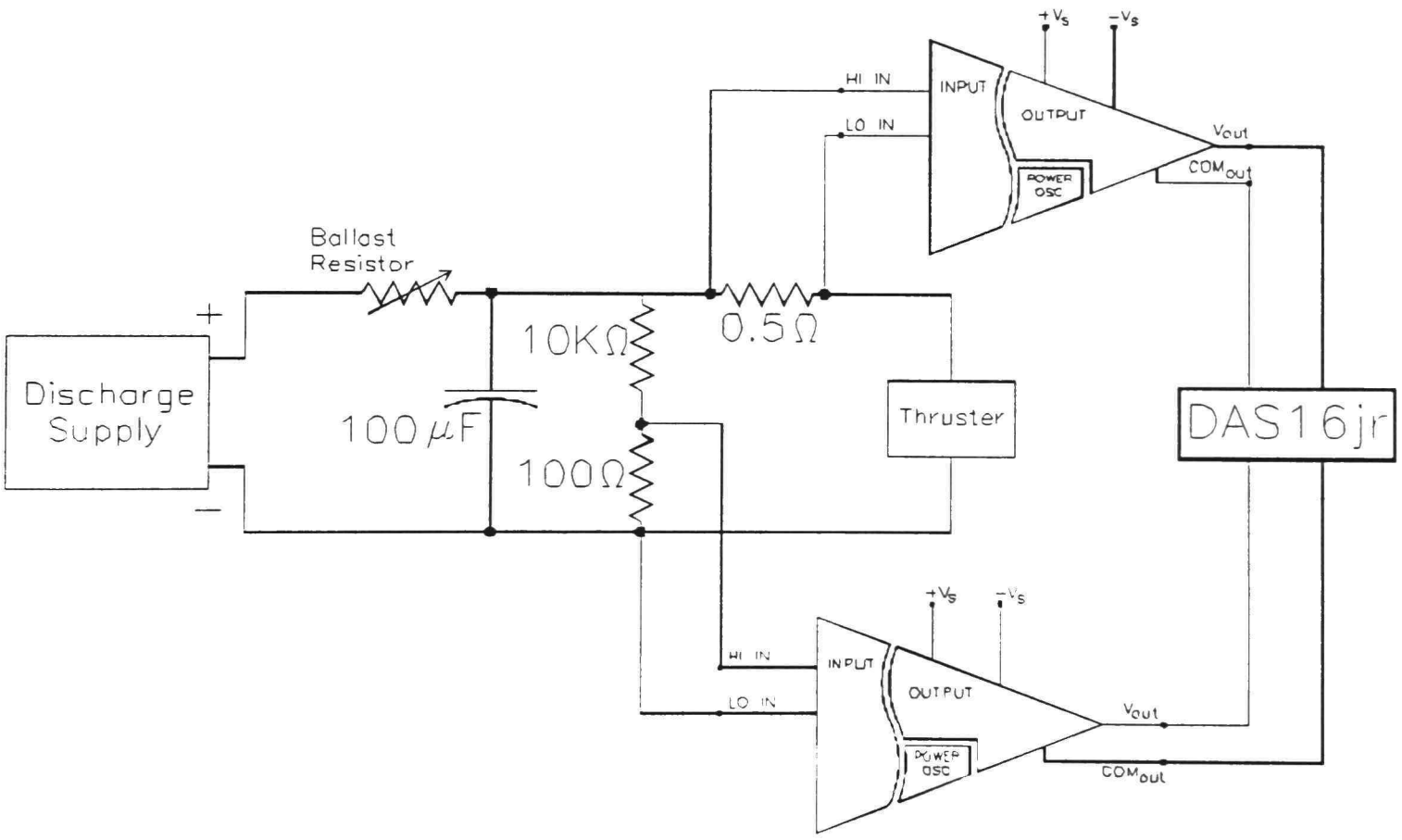

Figure 25 - Thruster anode voltage and current measurement setup

The signals received by the DAS16jr are used within the VisSim software. The sensors block in the main menu, Figure 20, receives these signals. Figure 26 is a schematic of the sensor block. Channel 3 of the DAS16jr receives the signal from the

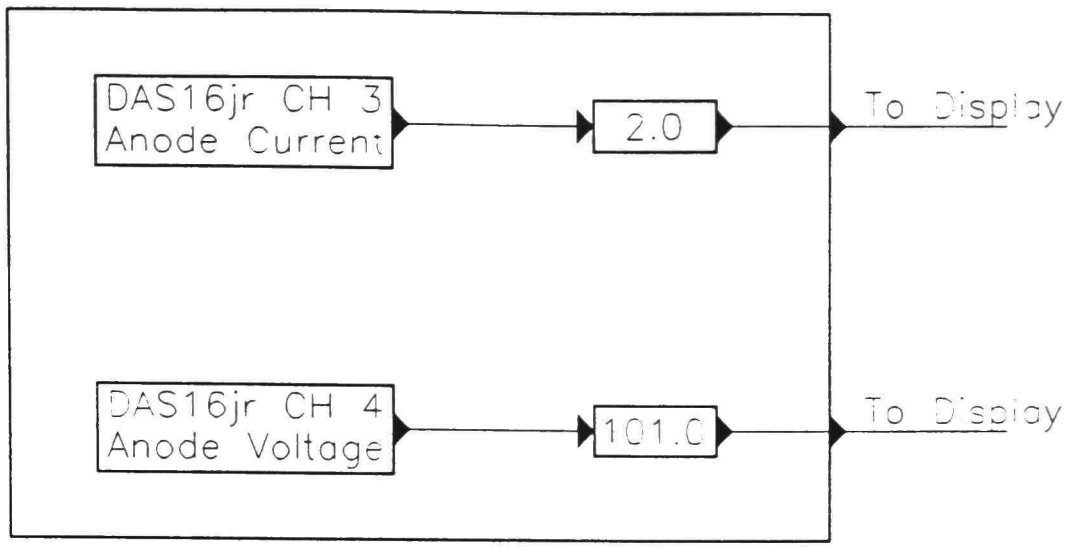

Figure 26 - Sensor compound block

0.5 Ω resistor. The signal is multiplied by a gain of 2.0. This is then displayed as the anode current. A similar method is used for displaying the anode voltage from the signal produced by the 100 Ω resistor.

The VisSim software is also used to monitor the mass flow of Xenon to the thruster. Outputs from the mfc power supply are fed directly to the DAS16jr, shown in Figure 27. These signals are used within VisSim to display the mass flow of the anode and cathode. Units refers to the brand name of the mfc power supply.

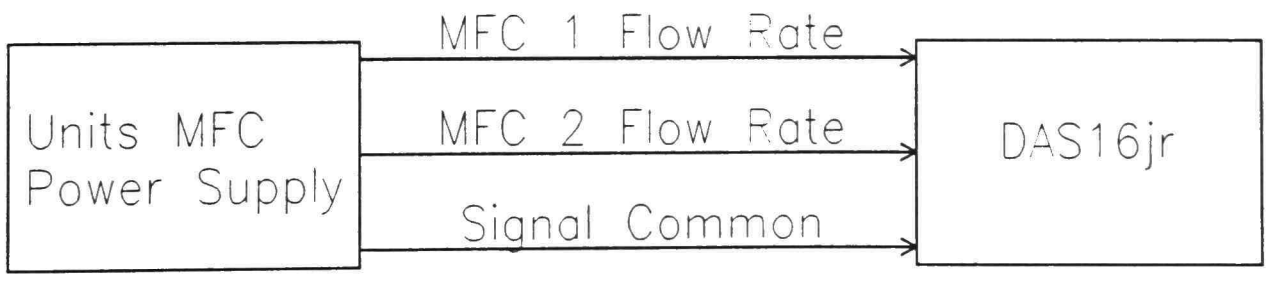

Figure 27 - Mass flow measurement setup

As mentioned earlier, the DAS16jr is capable of sampling at 1 megasample per second. However, the VisSim software is capable of recording samples at only 1 kilosample per second. Fortunately, this software was not required to record high speed data, but rather used only to monitor the parameters of the thruster during steady state

operation. The high speed data acquisition was performed by the Compuscope Lite A/D board and the Gagescope software.

Compuscope Lite A/D Board

Compuscope Lite[7] is a high speed, low cost, A/D board, shown in Figure 28, that is capable of sampling two channels simultaneously at 20 MSPS or one channel at 40 MSPS. Input impedance is 1 megaohm. Signal-to-noise ratio is 42 dB for a 1 MHz signal at 20 MSPS. Input range is +/- 1 volt and +/- 200 mV.

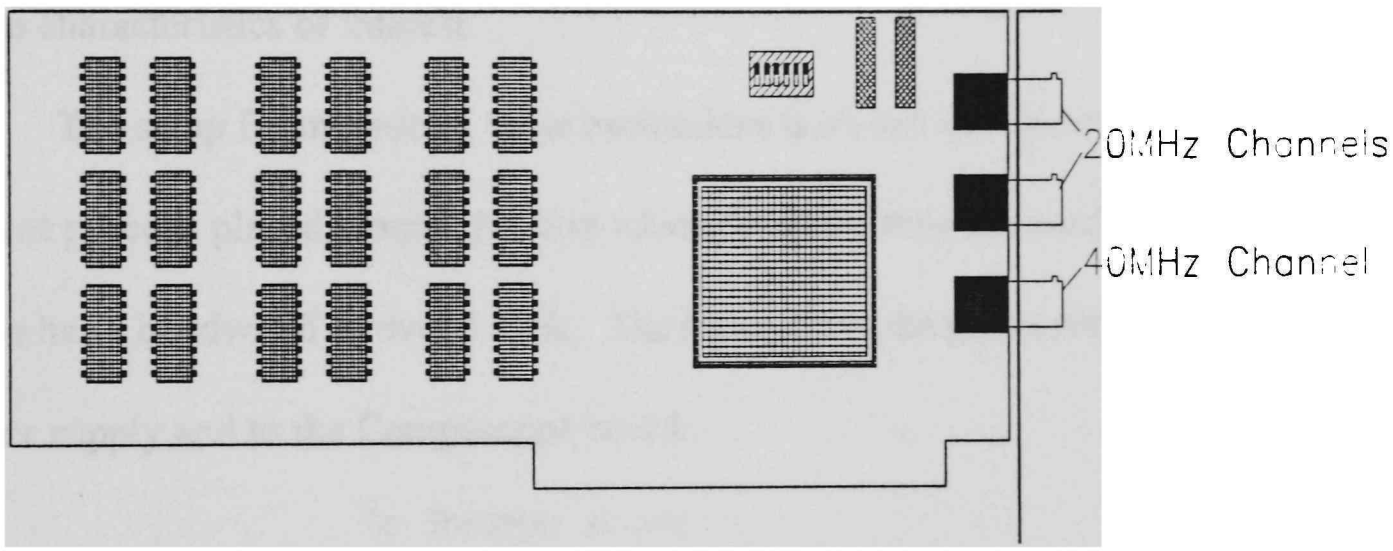

Figure 28 - Compuscope Lite A/D board

Gagescope software can be described as emulating an oscilloscope front panel. Options include multiple channels, high speed trigger view display that updates the screen as fast as 40 times per second, continuous capture, 16 kbytes of memory, and zoom capabilities.

The Nyquist Theorem states that a function, v(t), whose highest frequency component is f_{max}, must be sampled at a frequency F_s such that

$$Fs \geq 2 * fmax.$$

In other words, if an A/D device samples the input signal at a maximum frequency of F_s, the signal will not be reconstructed properly unless it is guaranteed that the maximum frequency component of the input signal is $0.5F_s$.

Current Probe

During normal operating modes, the Hall thrusters exhibit oscillations in the current flowing to the anode. Discharge current oscillations can vary from 20 kHz to 100 kHz depending on the type of Hall thruster and other factors. These oscillations are one of the characteristics of interest.

The setup for measuring these oscillations is shown in Figure 29. A Tektronix current probe is placed around the wire which feeds the thruster anode. The current probe has a bandwidth of over 1 GHz. The signal from the probe runs through the probe power supply and to the Compuscope board.

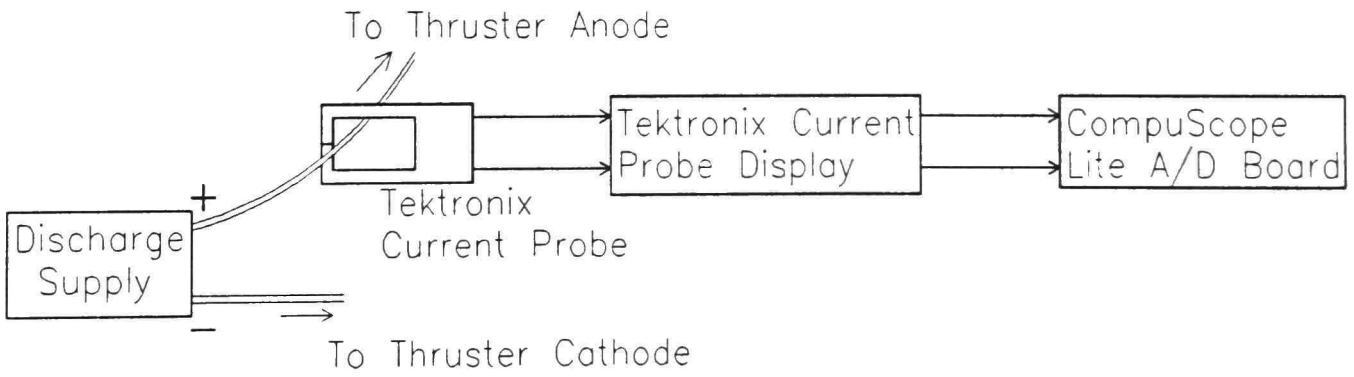

Figure 29 - Current oscillation measurement setup

Samples of current oscillations for each of the thrusters are shown in Figures 30 through 32. Data was taken during normal steady-state operation.

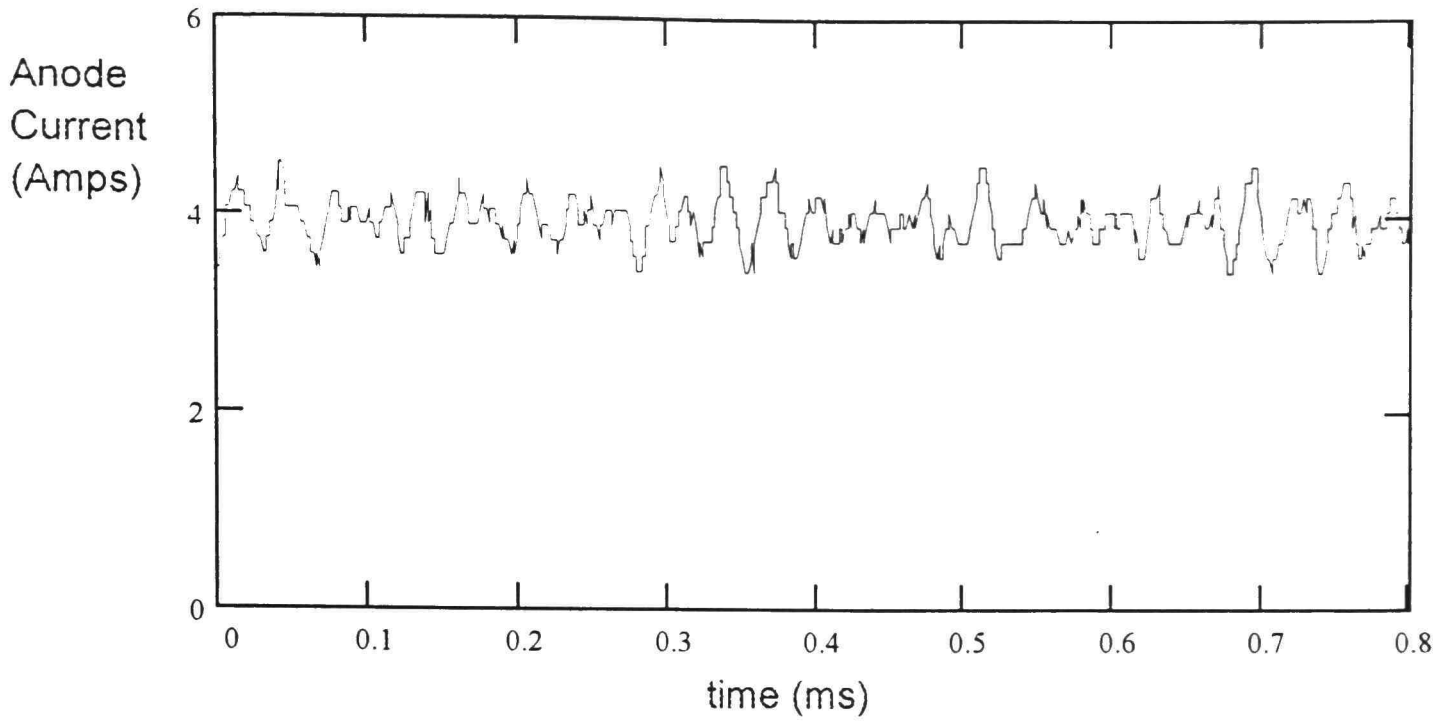

Figure 30 - Current oscillations of the D-55 at 300 V and 4.5 A

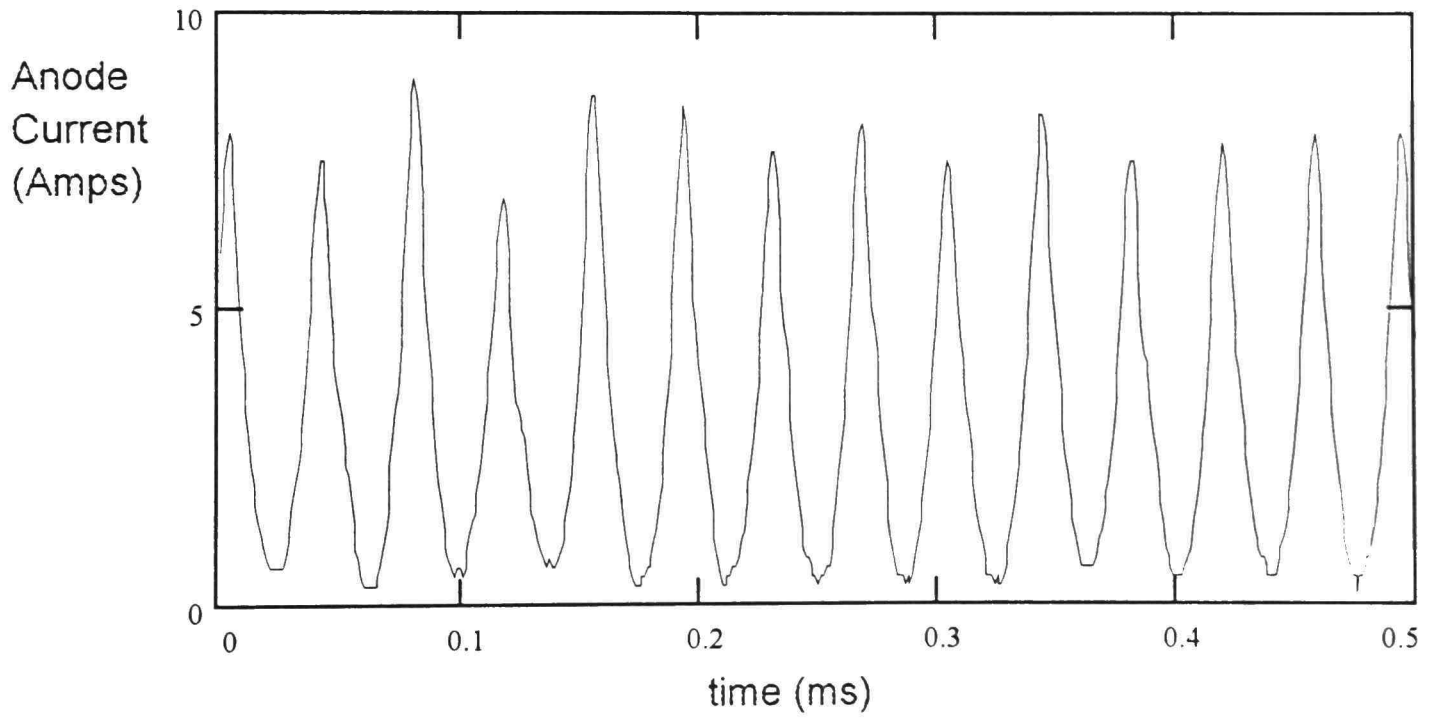

Figure 31 - Current oscillations of the SPT-100 at 300 V and 4 A

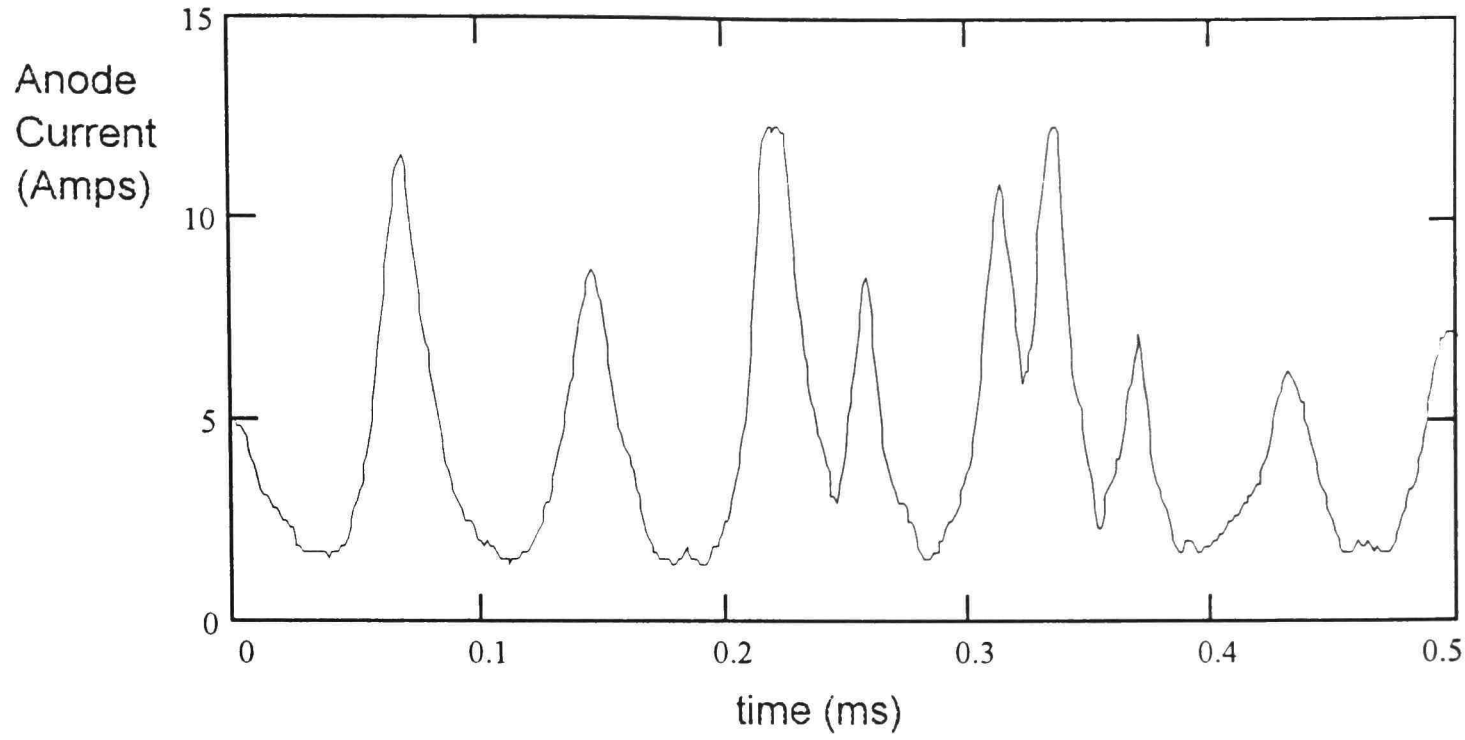

Figure 32 - Current oscillations of the T-100 at 300 V and 4.5 A

Care was taken to sample fast enough to prevent aliasing. The fastest current oscillations are those of the D-55, roughly 80 kHz. Therefore, samples were taken at a speed faster than 200 kSPS.

Another area of interest is the anode current during shutdown and startup of the thruster. Figure 33 displays the anode current of the D-55 during a typical shutdown and startup sequence. Since we were not concerned with the current oscillations, but rather the steady-state value, the aliasing effects were disregarded.

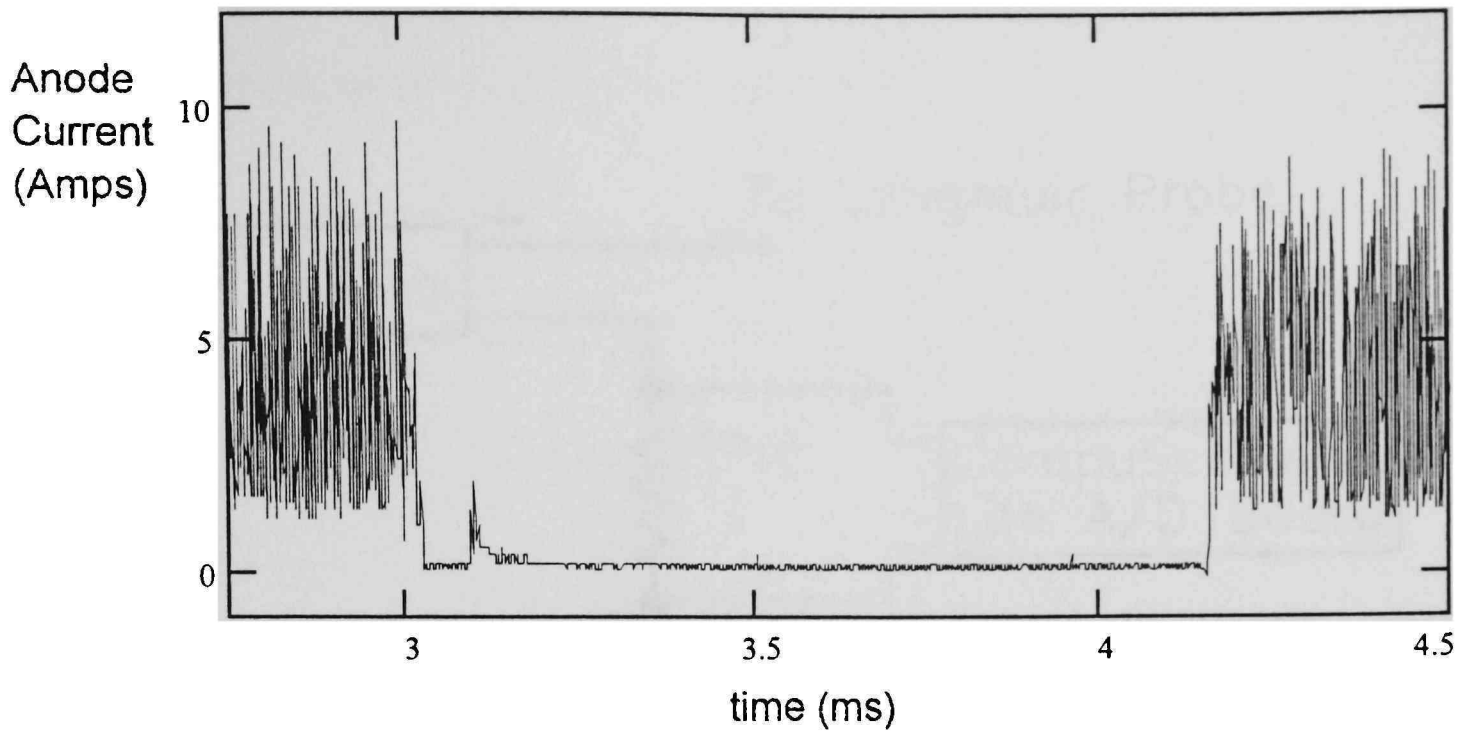

Figure 33 - Thruster start up current at 300 V and 4.5 A

Langmuir Probe

The Langmuir probe setup was similar to the type described by Myers and Manzella.[8] A cylindrical Langmuir probe was mounted on a cantilevered arm (refer back to Figure 4). The arm was mounted to a stepper motor. This made it possible to sweep the Langmuir probe 180 degrees about a radius of 40 cm. Since the thruster could not be mounted at the end of this radius, the varying distance of the probe from the exit plane of the thruster had to be accounted for. The Langmuir probe was a 1.57 cm long, 0.051 cm diameter piece of tungsten wire extending from a 1 mm outer diameter, 5 cm long alumina insulator.

The probe was biased relative to the tank wall using the circuit shown in Figure 34. The power supply placed the Langmuir probe at a positive potential of around 50 V. The probe current was measured using a 10 Ω shunt resistor. Isolation of the resistor

from the Compuscope board was unnecessary since one end of the resistor was grounded to the tank.

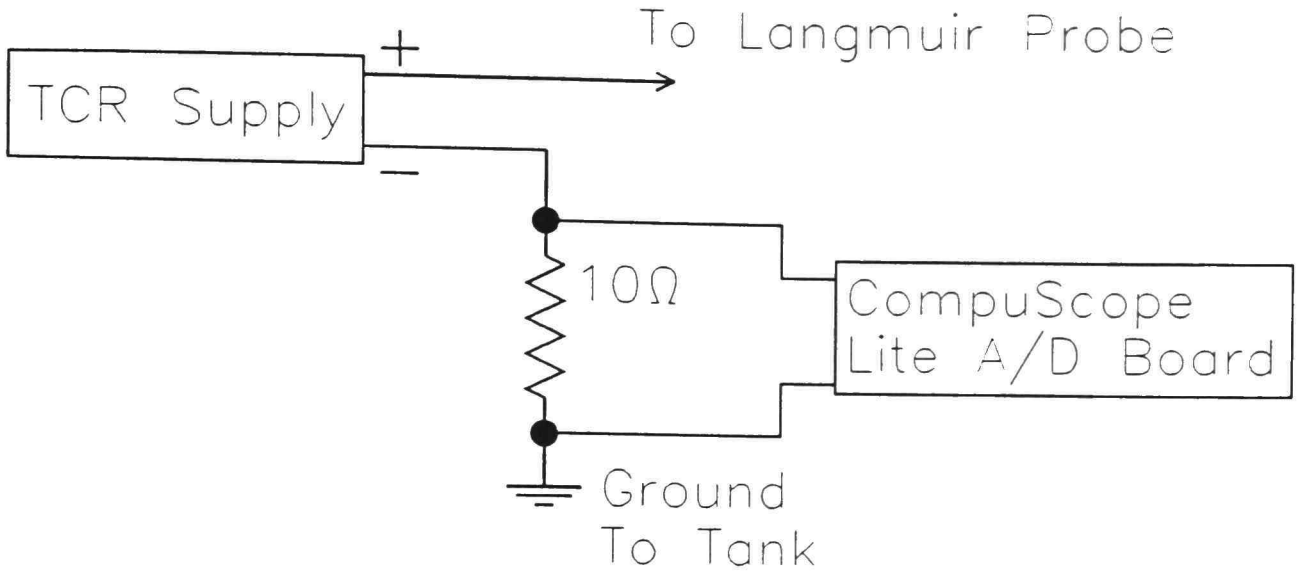

Figure 34 - Langmuir probe setup

According to thin sheath probe theory,[9] a general current-voltage characteristic curve for single probe operation is depicted in Figure 35.

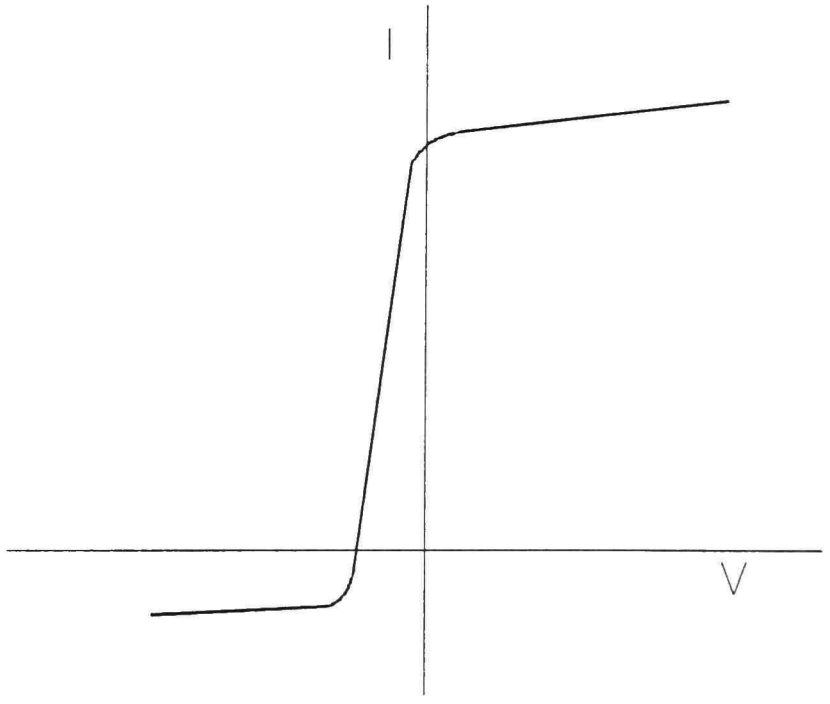

Figure 35 - General I-V characteristic for a Langmuir probe

The voltage on the probe was sufficient to place the I-V characteristic in the positive current saturation region. Therefore, fluctuations in plasma electron density will result in

correlating fluctuations of the probe current. Figure 36 shows probe current oscillations during steady state operation of the T-100 thruster.

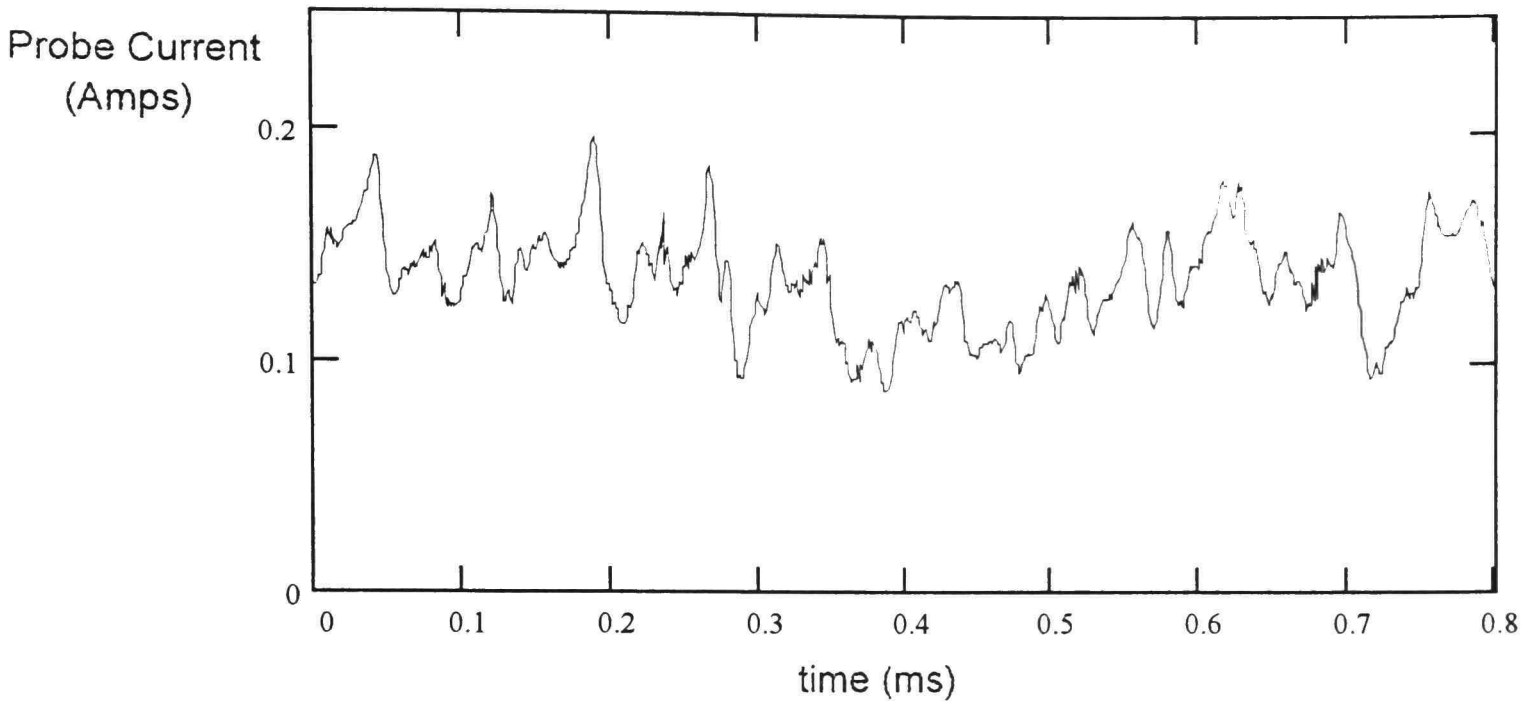

Figure 36 - Probe current oscillations of the T-100

Another thruster characteristic of interest was the exhaust plume. As mentioned earlier, the Langmuir probe was mounted on a cantilevered arm connected to a stepper motor. This made it possible to sweep the probe across the plume in approximately 7 seconds while maintaining a constant distance from the thruster. The probe current, shown in Figure 37, gave an approximation of the relative plasma density of a cross-section of the thruster plume during steady state operation.

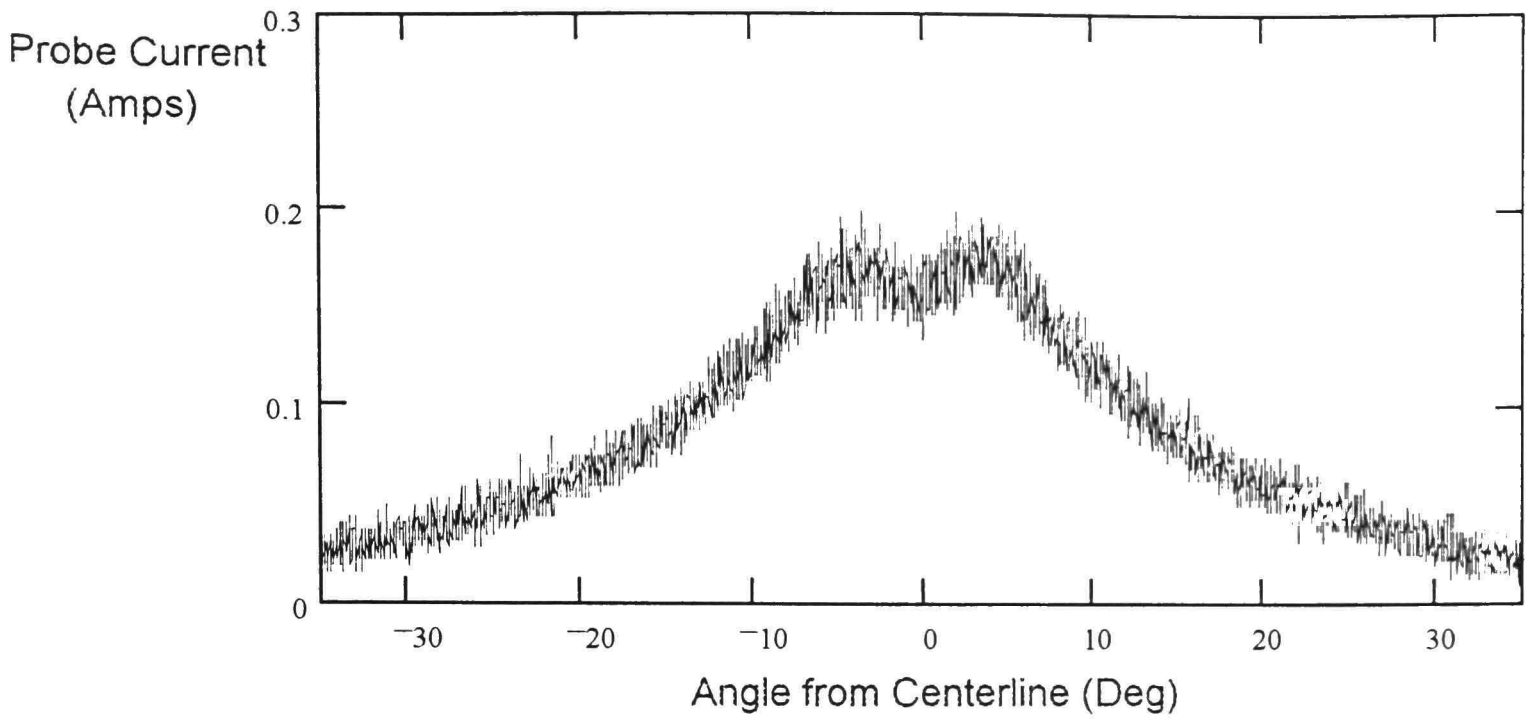

Figure 37 - Probe current during a sweep of the exhaust plume

CHAPTER V

CONCLUSIONS

A control and data acquisition system was built for the purpose of investigating characteristics of the Hall thruster. The control system consisted of a six channel D/A board, solid state relays, isolation amplifiers, and controls software all integrated by use of a 486 50 MHz computer.

The data acquisition system consisted of two A/D boards and two software packages. Characteristics investigated were current and plasma oscillations. This was achieved by use of current and Langmuir probes.

Several problems were discovered with the system after the initial assembly. Cables running from the power supplies to the computer induced small currents in the each other. Therefore, care was taken to properly ground and shield all cables. Another problem was the introduction of noise from the internal programming circuitry of the power supplies. In order to solve this problem, bypass capacitors were inserted where necessary. There was also a problem with the control software "freezing up" after several hours of use. This was corrected by increasing the RAM of the computer from 4 megabytes to 8 megabytes.

Once the system was assembled and debugged, it worked flawlessly. Over 100 hours were logged on the system without failure. The system is very flexible and could be used on other projects in the future.

REFERENCES

1. Anode Layer Thruster, Operating Instructions, Kaliningrad, Moscow Region, 1993.

2. Brophy, J. R., "Stationary Plasma Thruster Evaluation in Russia," JPL Publication 92-4, Mar. 1992.

3. CIO-DDA06 User's Manual, Computer Boards Inc., Mansfield, MA, 1991.

4. Analog Devices Data Converter Reference Manual, Analog Devices, Norwood, MA, 1994.

5. Vis Sim User's Guide, Visual Solutions Inc., Westford, MA, 1994.

6. CIO-AD16jr User's Manual, Computer Boards Inc., Mansfield, MA, 1991.

7. Gagescope Technical Reference and User's Guide, Montreal, Canada, 1993.

8. Myers, R. M., and Manzella, D. M., "Stationary Plasma Thruster Plume Characteristics," IEPC Paper 93-096. Proceedings of the 23rd International Electric Propulsion Conference, Sept. 1993.

9. Chung, P.M., Talbot, L., and Touryan, K.J., Electric Probes in Stationary and Flowing Plasmas, Applied Physics and Engineering Vol. II, Springer Verlag, New York, 1975.

PERMISSION TO COPY

In presenting this thesis in partial fulfillment of the requirements for a master's degree at Texas Tech University or Texas Tech University Health Sciences Center, I agree that the Library and my major department shall make it freely available for research purposes. Permission to copy this thesis for scholarly purposes may be granted by the Director of the Library or my major professor. It is understood that any copying or publication of this thesis for financial gain shall not be allowed without my further written permission and that any user may be liable for copyright infringement.

Agree (Permission is granted.)

John J. Mankowski — 5/8/95

Student's Signature — Date

Disagree (Permission is not granted.)

Student's Signature — Date